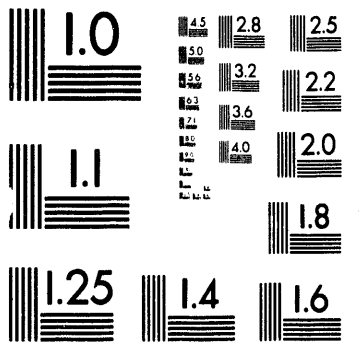
1.0
1.1
1.25
1.4
1.6
1.8
2.0
2.2
2.5
2.8
3.2
3.6
4.0
4.5
5.0
5.6
6.3
7.1

1 of 1

LBL-34124 Rev.

VORTEX METHODS[1]

Alexandre J. Chorin

Department of Mathematics and Lawrence Berkeley Laboratory
University of California
Berkeley, CA 94720

Presented at
Les Houches Summer School of Theoretical Physics
Les Houches, France
June 28–July 30, 1993

[1] This work was supported in part by the Applied Mathematical Sciences Subprogram of the Office of Energy Research, U.S. Department of Energy under Contract DE-AC03-76SF00098.

VORTEX METHODS

Alexandre J. Chorin
Department of Mathematics and Lawrence Berkeley Laboratory
University of California
Berkeley, CA 94720, USA

Table of Contents

1. Introduction: what are vortex methods?

Vortex methods originated from the observation that in incompressible inviscid flow vorticity (or, more accurately, circulation) is a conserved quantity, as can be readily deduced from the absence of tangential stresses. Thus, if the vorticity is known at time $t = 0$, one can find the flow at a later time by simply following the vorticity. In this narrow context, a vortex method is a numerical method that follows vorticity.

However, more generally, viscous flow problems have a Lagrangian, albeit stochastic, representation [C4],[G2],[L4]. Compressible flow has Lagrangian representations [L1]. More generally yet, in many problems there are variables such as charge, stellar or plasma mass, helicity, impulse, chemical species, that are transported either passively or modified

by known interactions; this transport/modification can be represented by following particles, or polygons, or domain boundaries; by moving particles, or by finite elements, finite differences, or boundary integrals. Lagrangian methods have a close resemblance to integral methods (see e.g. [G3]). Aspects of Lagrangian methods, such as particle creation at walls, have found application in non-Lagrangian methods (see e.g. [H5]). Fast summation methods, designed for particle methods, have found uses outside of computational physics.

Even more generally, the analysis of vortex methods leads, as we shall see, to problems that are closely related to problems in quantum physics and field theory, as well as in harmonic analysis. A broad enough definition of vortex methods ends up by encompassing much of science. Even the purely computational aspects of vortex methods encompass a range of ideas for which vorticity may not be the best unifying theme.

We shall restrict ourselves in these lectures to a special class of numerical vortex methods, those that are based on a Lagrangian transport of vorticity in hydrodynamics by smoothed particles ("blobs") and those whose analysis contributes to the understanding of blob methods. Blob methods started in the thirties as two-dimensional "point" methods [R3]. By the fifties, it was discovered that "point vortex" methods had drawbacks, and a misinterpretation of the Poincaré recurrence theorem led to the conclusion that the drawbacks could not be remedied (for an analysis, see [K7]). In the late sixties and early seventies, the virtues of smoothing were discovered [C3],[C4],[C12] and viscosity and boundaries were added.

The generalization to three dimensions followed soon [C5],[L2],[L3], and was found to be non-unique. Arrows, filaments, dipoles, magnets, all generalize two-dimensional blobs,

and we shall compare them below. All three-dimensional inviscid blob methods eventually lose stability; the analysis of that instability requires a deeper understanding of turbulence and contributes to the understanding of quantum fluids.

Are vortex methods good numerical methods? The answer is time-dependent and problem dependent. Vortex methods made possible pioneering investigations of vortex sheets [K6],[K7],[T1], high Reynolds number wakes [C2], and various three-dimensional problems involving vortex rings, jets, and wakes (see e.g. [A5],[K4],[M4]). As time progressed, other methods caught up with some of these applications, but then vortex methods also improved. Vortex methods (i.e., "blob" methods) are a very useful part of the panoply of computational fluid mechanics, but do not exhaust it. An important class of vortex methods are "hybrids", which borrow some of the devices of vortex methods and couple them with other ideas [C17],[R4],[W1]. Good examples are the methods developed recently by Cottet, in which a finite difference method is used near boundaries to resolve boundary layers, while a vortex method is used far from the wall to ensure the correct transport of vorticity. Another class of methods, first implemented by Shestakov, uses finite differences in the interior and vortices near walls; it has been recently suggested by Bernard that in some problems such methods can obviate the need for extraordinarily fine resolution and very small time steps near walls that bedevils finite difference methods used alone. I shall disregard here all hybrids, but advise the numerical analyst to keep them in mind.

I will put some emphasis on a more arcane use of vortex methods. Vortex methods for inviscid flow lead to systems of ordinary differential equations that can be readily cast in

Hamiltonian form, both in three and two space dimensions, and they can preserve exactly a number of invariants of the Euler equations, including topological invariants. Their viscous versions resemble Langevin equations. As a result, they provide a very useful cartoon of statistical hydrodynamics, i.e., of turbulence, one that can to some extent be analyzed analytically and, more importantly, explored numerically, with important implications also for superfluids, superconductors, and even polymers. In my view, vortex methods provide the most promising path to the understanding of these systems.

Before launching in the description of vortex methods, I would like to say a few words of caution. Vortex methods operate with objects, vortices, that have a clear physical interpretation. Nature is rife with vortices, (tornadoes, hurricanes, ...), and it is very tempting to identify the numerical objects with physical ones. This near-physicality has many attractions, but also some dangers. A vortex method produces easily results that look plausible to the naked eye, or when presented on a videotape. Such results are not necessarily accurate. People have tried to model, say, turbulent boundary layers, with a few dozen vortex elements, while being aware that a spectral calculation would require millions of unknowns to yield useful results in the same problem. Even the wildest proponent of vortex methods will not suggest that a vortex method can give something useful with no effort.

One should in particular draw a clear distinction between numerical approximation by vortex methods (the main subject of these talks) and physical modelling based on a vortex representation. I shall give below some examples of the modelling mode, in the context of vortex lattices. Modelling and approximation are different; in particular, the vortex cores

needed for accuracy are designed on the basis of an analysis of approximation kernels; they are not normally meant to be "physical". I shall give below an example of a core designed on the basis of physical models; it is not useless, but it is not as accurate as cores designed by mathematical analysis. For accuracy, a physical vortex must be approximated by a cloud of numerical vortices, or else the results will be quantitatively wrong (if occasionally qualitatively beguiling). The confusion between vortex-based modelling and vortex-based numerical methods is the origin of many misunderstandings.

2. Vortex methods in the plane.

We begin with a description of vortex methods for two-dimensional inviscid unbounded flow.

Consider a velocity field $\mathbf{u}(\mathbf{x},t)$, $\mathbf{u}=(u_1,u_2)$, where $\mathbf{x}=(x_1,x_2)$ is the position vector and t is the time. First, pick a fixed point $\mathbf{x}$, and consider the points in the plane within a distance h of $\mathbf{x}$, i.e., $\mathbf{x}=\mathbf{x}+\mathbf{h}$, $\mathbf{h}=(h_1,h_2)$, $h=|\mathbf{h}|$ = length of $\mathbf{h}$, small enough so that h^2 is negligible. Then

$$u_1(\mathbf{x}+\mathbf{h}) \cong u_1(\mathbf{x}) + h_1\partial_1 u_1 + h_2\partial_2 u_1, \qquad \partial_1 \equiv \tfrac{\partial}{\partial x_1},$$

$$u_2(\mathbf{x}+\mathbf{h}) \cong u_2(\mathbf{x}) + h_1\partial_1 u_2 + h_2\partial_2 u_2,$$

or

$$\mathbf{u}(\mathbf{x}+\mathbf{h}) = \mathbf{u}(\mathbf{x}) + (\nabla u)\mathbf{h},$$

where (∇u) is the matrix with entries $(\nabla u)_{ij} = \partial_i u_j$, $i=1,2$, $j=1,2$. Let $D = \frac{1}{2}\left((\nabla u)+(\nabla u)^T\right)$ (T denotes a transpose) be the deformation matrix. Then

$$(\nabla u)\mathbf{h} = \mathrm{grad}_h(D\mathbf{h},\mathbf{h}) + \frac{1}{2}\boldsymbol{\xi}\times\mathbf{h},$$

where

$$\begin{aligned} \mathrm{grad}_h(D\mathbf{h},\mathbf{h}) &= (\partial_{h_1}(D\mathbf{h},\mathbf{h}),\partial_{h_2}(D\mathbf{h},\mathbf{h}))\,, \\ \boldsymbol{\xi} &= (0,0,\xi), \quad \xi = \partial_2 u_1 - \partial_1 u_2, \\ \mathbf{h} &= (h_1,h_2,0). \end{aligned}$$

(Note that $\boldsymbol{\xi}$ is a three-dimensional vector pointing out of the plane of the motion.) It is easy to see that the velocity field $\mathrm{grad}_h(D\mathbf{h},\mathbf{h})$ represents a deformation, and $\frac{1}{2}\boldsymbol{\xi}\times\mathbf{h}$ represents a rotation with angular velocity $\frac{1}{2}\xi$. Thus the most general motion of a fluid can be locally written as the sum of a solid body translation, a deformation, and a rotation with angular velocity $\frac{1}{2}\xi$; ξ is the vorticity.

An ideal fluid is, by definition, a fluid which cannot support tangential forces. Rotation can then be neither started nor stopped, and one expects ξ to be a privileged variable. Indeed, the Euler equations for an incompressible fluid can be written as

$$\partial_t\mathbf{u} + (\mathbf{u}\cdot\nabla)\mathbf{u} = -\mathrm{grad}\ p \tag{1a}$$

$$\mathrm{div}\ \mathbf{u} = 0. \tag{1b}$$

where p is the pressure and ∇ the differentiation vector. Taking a curl, one obtains

$$\partial_t\xi + (\mathbf{u}\cdot\nabla)\xi = 0,$$

or

$$\frac{D\xi}{Dt} = 0, \tag{2}$$

where $D/Dt \equiv \partial_t + \mathbf{u}\cdot\nabla$ denotes differentiation following a particle. Vorticity is thus conserved.

Another consequence of the equation of motion is the following: Let C be a closed contour in the plane; let C_t be its image under the flow (i.e., the locus of points that C reaches after a flow during the time t). Then

$$\int_C \mathbf{u}(\mathbf{x},0)\cdot d\mathbf{s} = \int_{C_t} \mathbf{u}(\mathbf{x},t)\cdot d\mathbf{s};$$

this invariant, the circulation along C, will be denoted by Γ_C. (The three-dimensional analogue of this result also holds.) Note

$$\int_C \mathbf{u}\cdot d\mathbf{s} = \int_\Sigma \boldsymbol{\xi}\cdot d\Sigma,$$

where Σ is the interior of C.

The equation div $\mathbf{u} \equiv \partial_1 u_1 + \partial_2 u_2 = 0$ is the statement of incompressibility. As its consequence, there exists a function ψ, the stream function, such that $u_1 = \partial_2\psi$, $u_2 = -\partial_1\psi$. Substitution into the definition of ξ yields

$$\Delta\psi = -\xi, \quad \Delta = \text{Laplace operator} \equiv \partial_1^2 + \partial_2^2.$$

Let $G(\mathbf{x},\mathbf{x}') = G(\mathbf{x}-\mathbf{x}')$ be the Green function for the Laplace operator; $\Delta G = \delta(\mathbf{x}-\mathbf{x}')$; $G = -\frac{1}{2\pi}\log|\mathbf{x}-\mathbf{x}'|$, where $|\mathbf{x}|$ denotes the length of the vector $\mathbf{x}$. $\Delta\psi = -\xi$ then implies $\psi = \frac{1}{2\pi}\int \log|\mathbf{x}-\mathbf{x}'|\xi(\mathbf{x}')d\mathbf{x}'$, where $d\mathbf{x} \equiv dx_1 dx_2$, and then $\mathbf{u} = (\partial_2, -\partial_1)\psi = \frac{1}{2\pi}\int \begin{pmatrix} \partial_2 \\ -\partial_1 \end{pmatrix} \log|\mathbf{x}-\mathbf{x}'|\ \xi(\mathbf{x}')d\mathbf{x}'$.

Introduce the notation

$$f * g \equiv \int f(\mathbf{x}-\mathbf{x}')g(\mathbf{x}')d\mathbf{x}',$$

$f * g$ is the convolution of f and g. For later reference, note:

$$\begin{aligned} f * g &= g * f, \\ f * \delta &= f, \quad \delta = \text{Dirac delta function}, \end{aligned}$$

and

$$D(f * g) = (Df * g) = (f * Dg),$$

for any differentiation operator D and whenever the expressions make sense. Thus,

$$\mathbf{u} = K * \xi,$$

where $K = \frac{1}{2\pi} \begin{pmatrix} \partial_2 \\ -\partial_1 \end{pmatrix} \log |\mathbf{x}| = \frac{1}{2\pi} \left(\frac{-x_2}{r^2}, \frac{x_1}{r^2} \right)$, $r^2 = x_1^2 + x_2^2$.

Given any point in the fluid, located initially at $\boldsymbol{\alpha}$, its subsequent motion is given by

$$\frac{d\mathbf{x}}{dt} = \mathbf{u}(\mathbf{x}, t), \quad \mathbf{x}(0) = \boldsymbol{\alpha}. \tag{3}$$

Let supp ξ denote the support of ξ, i.e., the set of points where $\xi \neq 0$. Take a point $\boldsymbol{\alpha}$ in supp ξ. The motion of that point will also follow (3), with the attached vorticity unchanged. If one considers an infinite number of equations, one per point in supp ξ, one obtains the motion of the vorticity (since $\xi(\mathbf{x}(\mathbf{t})) = \xi(\boldsymbol{\alpha})$ if $\mathbf{x}(0) = \boldsymbol{\alpha}$, by the conservation of vorticity); ξ gives rise to $\mathbf{u}$ by $\mathbf{u} = K * \boldsymbol{\xi}$, and the Euler equations are solved. To discretize this system for computer use, one can take a finite number of initial points $\boldsymbol{\alpha}_1, \ldots, \boldsymbol{\alpha}_N$, and solve the finite set of ordinary differential equations

$$\begin{aligned} \frac{d\mathbf{x}_i}{dt} &= K * \xi, \quad i = 1, \ldots, N, \\ \mathbf{x}_i(0) &= \boldsymbol{\alpha}_i, \end{aligned}$$

where ξ on the right-hand side is attached to the moving points, i.e., $\xi = \sum_{i=0}^{N} \tilde{\xi}_i \delta(\mathbf{x} - \mathbf{x}_i)$, δ = Dirac delta, and the $\tilde{\xi}_i$ are some appropriate constants. It is natural to require that $\sum \tilde{\xi}_i = \int \xi(\mathbf{x}) d\mathbf{x}$. Then

$$\frac{d\mathbf{x}_i}{dt} = \sum_{j \neq i} K(\mathbf{x}_i - \mathbf{x}_j) \tilde{\xi}_j$$

(the term $i = j$ is excluded to avoid a singularity), or

$$\begin{aligned} \frac{dx_i}{dt} &= -\sum_{j \neq i} \frac{1}{2\pi} \frac{(y_i - y_j)}{r_{ij}^2} \tilde{\xi}_j \qquad r_{ij}^2 = (x_i - x_j)^2 + (y_i - y_j)^2 \\ \frac{dy_i}{dt} &= \sum_{j \neq i} \frac{1}{2\pi} \frac{(x_i - x_j)}{r_{ij}^2} \tilde{\xi}_j \qquad \tilde{\xi}_j = \text{constants.} \end{aligned} \tag{4}$$

Where $x = x_1, y = x_2$ for the sake of clarity. This is the point vortex method, which converges, though not very fast [H4],[K7]. Its flaws can be seen by considering two nearly "point" vortices (vorticity functions of the form $\tilde{\xi}_i \delta(\mathbf{x} - \mathbf{x}_i)$). Equations (4) will cause them to rotate around each other very fast. Such "trapping" is indeed a physical process for isolated vortices, but the intensity of the rotation that results is unreasonable. The "point" approximation must be smoothed. A plausible smoothing [C3],[C4] consists in replacing r_{ij}^2 by $r_{ij}\epsilon$ for $r_{ij} \leq \epsilon$. A more general smoothing can be obtained [H1],[B2] by changing K to K_ϵ, where $K_\epsilon = K * \phi_\epsilon$, with ϕ_ϵ a smooth function of small support (i.e., vanishing over most of the plane except near the origin). K_ϵ is then smooth, and the result is a smoothing of equations (4). In general, we shall pick ϕ_ϵ so that

$$\phi_\epsilon = \epsilon^{-2} \phi(\mathbf{x}/\epsilon), \qquad \phi \text{ smooth},$$

$$\int \phi(\mathbf{x}) d\mathbf{x} = 1,$$

$$\int x_1^{\alpha_1} x_2^{\alpha_2} \phi(\mathbf{x}) d\mathbf{x} = 0 \qquad \text{for } \alpha_1 \geq 0,\ \alpha_2 \geq 0,\ \alpha_1 + \alpha_2 \leq p - 1,$$

where p is an integer to be chosen. Recipes for choosing p and constructing ϕ will be given below (see also [B2],[B4],[H1],[H2]). Note that changing $K \rightarrow K_\epsilon$ is identical to keeping K but changing $\tilde{\xi}\delta(\mathbf{x} - \mathbf{x}_i)$ into $\tilde{\xi}\phi_\epsilon(\mathbf{x} - \mathbf{x}_i)$, i.e., to smearing vortex points into vortex "blobs".

It will turn out that the accuracy of the smoothed method depends on p. In the absence of walls, we shall see that it is reasonable to choose the initial $\boldsymbol{\alpha}_i$ on a regular grid, and choose $\tilde{\xi}_i$ to be the initial values of $\xi(\mathbf{x})$ at these points, multiplied by a squared mesh size. The vortex method for an inviscid plane unbounded flow is now fully described, except for the general construction of ϕ. The recipe $r_{ij}^2 \rightarrow r_{ij}\epsilon$ for $r_{ij} \leq \epsilon$ is quite adequate for starting a calculation; the integration in time requires accuracy, but the system is not stiff and Runge-Kutta will do well; most programs seem to be using fourth-order Runge-Kutta.

There are other strategies for smoothing "point" methods. One can for example transport points in the support of ξ, and assume that ξ between the points is given by a polynomial distribution on a set of polygons. New polygons can be found as the geometry of the points changes. The integral of a polynomial times the kernel K on a polygon can be evaluated analytically and simply, yielding a simple and accurate "smoothed" method for transporting the points, one that can be made adaptive and is particularly efficient if the variation of ξ on its support is small [B7],[R4]. This is the "polygonal" vortex method.

What has a vortex method bought you that a simple finite difference integration of equation (4) does not provide? Note that the Navier-Stokes equations, to be discussed next, are formed by adding to the Euler equation higher derivatives multiplied by what is

usually a small coefficient. The error term in finite-difference or finite-element solutions of the Euler equations has the same form, producing numerical viscosity (and dispersion). The error in vortex methods has a different structure, because there is no differencing of the advection terms in space. This opens the door to a realistic analysis of the effect of a small viscosity.

Here too a note of caution is appropriate: if a calculation does not contain enough computational elements to represent a given phenomenon, the phenomenon will not be seen. One cannot represent, say, twenty waves with two vortices. As the Reynolds number is increased the complexity of the phenomena produced usually grows, especially in three dimensions. The number of computational elements must then increase or the complexity of the phenomena must be reduced by modelling, with a vortex method as with any other.

It is worth noting that equations (4) form a Hamiltonian system. They can be rewritten in the form

$$\tilde{\xi}_i \frac{dx_i}{dt} = -\frac{\partial H}{\partial y_i},$$
$$\tilde{\xi}_i \frac{dy_i}{dt} = -\frac{\partial H}{\partial x_i},$$

where $H = -\frac{1}{4\pi}\sum_i \sum_{j\neq i} \tilde{\xi}_i \tilde{\xi}_j \log|\mathbf{x}_i - \mathbf{x}_j|$. A simple scaling of the variables removes the factors $\tilde{\xi}_i$ on the left-hand side of these equations. Note that the Hamiltonian system is rather odd: the variable dual to one coordinate of a vortex is the other coordinate (rather than some momentum variable). If $K \to K_\epsilon$, the corresponding Hamiltonian has a smoothed interaction replacing the log. A short calculation shows that the Hamiltonian H differs from the kinetic energy $\frac{1}{2}\int \mathbf{u}^2 d\mathbf{x}$ by a constant (that is infinite if $\epsilon = 0$).

3. The Navier-Stokes equations in the plane.

The Navier-Stokes equations in the plane take the form

$$\frac{D\xi}{Dt} = R^{-1}\Delta\xi, \quad \text{div } \mathbf{u} = 0, \tag{5}$$

where R is the Reynolds number (that we assume is large), and as before, $\xi = \text{curl } \mathbf{u}$, $\mathbf{u} = K * \xi$.

Note that, while in a finite difference method one calculates the change in solution at fixed spatial points, in a vortex method one follows the motion in space of particles that carry a fixed value of the vorticity. The problem at hand is to couple this "particle" method to a diffusion with diffusion coefficient R^{-1}. We shall first discuss how this can be done in a "fractional step" method; a more general formulation will follow.

Consider a differential equation of the form

$$u_t = Au + Bu, \qquad u(0) = u_0,$$

where A, B are operators (for example, $A = \partial_1$, $B = \partial_1^2$). Its solution produces a "solution operator", i.e., an operator S_{A+B} such that

$$u(t) = S_{A+B}(t)u_0.$$

Let S_A, S_B be the solution operators of the equations $u_t = Au$, $u_t = Bu$ respectively, i.e.,

$$u_t = Au, \quad u(0) = u_0 \longleftrightarrow u(t) = S_A(t)u_0,$$

$$u_t = Bu, \quad u(0) = u_0 \longleftrightarrow u(t) = S_B(t)u_0,$$

where $\longleftrightarrow$ denotes an equivalence under the appropriate solvability conditions. Then, under quite general conditions, the Trotter ("fractional step") formula holds:

$$S_{A+B}(t) = \lim_{n\to\infty} \left(S_A\left(\frac{t}{n}\right) S_B\left(\frac{t}{n}\right)\right)^n,$$

i.e., one can solve the "partial" equations for short time intervals and combine the results to obtain the solution of the full problem [C13]. The error, i.e., the norm $\| S_{A+B}(t) - \left(S_A\left(\frac{t}{n}\right) S_B\left(\frac{t}{n}\right)\right)^n \|$ for finite n is typically $O(n^{-1})$, unless A and B commute or special precautions have been taken, when the error can become $O(n^{-2})$.

If one rewrites the Navier-Stokes equations as

$$\partial_t \xi = -(\mathbf{u}\cdot\nabla)\xi + R^{-1}\Delta\xi,$$

then the first partial equation is the Euler equation, and all one has to do is couple the vortices to a solution of the heat equation implemented on the moving vortex grid. Various successful ways of doing so are available [C15],[C17],[F1]. We shall present here the random version of such an algorithm; this was the first successful viscous vortex method [C4], and is of some interest in statistical mechanical models. As will emerge from our analysis, this random method is useful numerically only when R is large and a boundary is present. We begin with a little probability theory.

The possible outcomes of an experiment (such as throwing a die) form the points in a sample space S. A subset E of S is called an event. We assume that to each event is assigned a probability $P(E)$, a number between 0 and 1 which intuitively represents the fraction of times an outcome in E will occur if the experiment is repeated many times.

We assume, therefore, that $P(S) = 1$. Moreover, if two events E_1 and E_2 are disjoint, i.e., $E_1 \cap E_2 = \emptyset$, then $P(E_1 \cup E_2) = P(E_1) + P(E_2)$. Two events, E_1 and E_2 are called independent if

$$P(E_1 \cap E_2) = P(E_1) \cdot P(E_2)$$

Intuitively, two events are independent if the occurrence of one of them has no effect on the probability of the occurrence of the other one. (For instance, in the toss of two dice marked #1 and #2, the events "a two on #1" and "a three or a four on #2" are independent.)

A random variable is a number attached to the outcome of an experiment. The expectation or mean of η is defined by

$$\langle \eta \rangle = \int_S \eta dP.$$

For instance, if $S = \{s_1, \ldots, s_N\}$ and the probability of s_i occurring is p_i, then

$$\langle \eta \rangle = \sum_{i=1}^{n} \eta(s_i) p_i.$$

Suppose there is a function f on the real line such that the probability of η lying between a and b is $\int_a^b f(x)dx$. Then we say that η has the probability density function f. Clearly, $\int_{-\infty}^{\infty} f(x)dx = 1$. Also, one can show that

$$\langle \eta \rangle = \int_{-\infty}^{\infty} x f(x) dx.$$

The variance of η is defined by

$$\mathrm{Var}(\eta) = \langle (\eta - \langle \eta \rangle)^2 \rangle = \langle \eta^2 \rangle - \langle \eta \rangle^2$$

and the standard deviation by

$$\sigma(\eta) = \sqrt{\mathrm{Var}(\eta)}.$$

Two random variables, η_1 and η_2 are called independent if for any two sets A_1, A_2 in the real line, the events

$$\{s \in S | \eta_1(s) \in A_1\} \quad \text{and} \quad \{s \in S | \eta_2(s) \in A_2\}$$

are independent. For independent random variables, one has

$$\langle \eta_1 \eta_2 \rangle = \langle \eta_1 \rangle \langle \eta_2 \rangle$$

and

$$\mathrm{Var}(\eta_1 + \eta_2) = \mathrm{Var}(\eta_1) + \mathrm{Var}(\eta_2).$$

(From the definition, $\langle \eta_1 + \eta_2 \rangle = \langle \eta_1 \rangle + \langle \eta_2 \rangle$ is always true.)

The law of large numbers states that if $\eta_1, \eta_2, \ldots, \eta_2$ are random variables that are independent and have the same mean and variance as η, then

$$\langle \eta \rangle = \lim_{n \to \infty} \frac{1}{n} \sum_{i=1}^{n} \eta_i.$$

Part of the theorem is that the right-hand side is a constant. This result justifies our intuition that $\langle \eta \rangle$ is the average value of η when the experiment is repeated many times. The significance of the standard deviation is illuminated by Tchebysheff's inequality: If σ is the standard deviation of η,

$$P\left(\{s \in S | |\eta(s) - \langle \eta \rangle| \geq k\sigma\}\right) \leq \frac{1}{k^2}$$

for any number $k > 0$. For example, the probability that η will deviate from its mean by more than two standard deviations is at most $1/4$.

If a random variable η has the probability density function

$$f(x) = \frac{1}{\sqrt{2\pi\sigma^2}} e^{-(x-a)^2/2\sigma^2}$$

we say that η is gaussian. One can check that $\langle \eta \rangle = a$ and $\mathrm{Var}(\eta) = \sigma^2$. If η_1 and η_2 are independent gaussian random variables, then $\eta_1 + \eta_2$ is gaussian as well.

Next we show how gaussian random variables can be used in the study of the heat equation:

$$v_t = \nu v_{xx}, \qquad -\infty < x < \infty, \quad \geq 0.$$

Here v represents the temperature as a function of x and t, and ν represents the conductivity. If v is given at $t = 0$, then the heat equation determines it for $t > 0$. If initially $v(x, 0) = \delta(x)$, a delta function at the origin, then the solution of the heat equation is given by

$$H(x,t) = \frac{1}{\sqrt{4\pi\nu t}} \exp\left(\frac{-x^2}{4\nu t}\right). \tag{6}$$

This is the Green function for the heat equation (see any textbook on partial differential equations).

We can interpret the function (6) from a probabilistic point of view as follows: Fix time at t, and place N particles at the origin. Let each of the particles "jump" by sampling the gaussian distribution with mean zero and variance $2\nu t$. Thus, the probability that a particle will land between x and $x + dx$ is

$$\frac{1}{\sqrt{4\pi\nu t}} \exp\left(\frac{-x^2}{4\nu t}\right) dx.$$

If we repeat this with a large number of particles, we find

$$\lim_{N\to\infty} \frac{\text{number of particles between } x \text{ and } x+dx \text{ at time } t}{N\ dx} = \frac{1}{\sqrt{4\pi\nu t}}\exp\left(\frac{-x^2}{4\nu t}\right).$$

Next consider the solution $v(x,t)$ of the heat equation with given initial data $v(x,0) = g(x)$. The solution is

$$v(x,t) = \int_{-\infty}^{\infty} H(x,x',t)g(x')dx', \tag{7}$$

where

$$H(x,x',t) = \frac{1}{\sqrt{4\pi\nu t}}\exp\left(\frac{-(x-x')^2}{4\nu t}\right).$$

This general solution has a probabilistic interpretation as well. Instead of starting N particles at the origin, start N randomly spaced particles on the line, at positions, say x_i^0, $i = 1,\ldots,N$, and assign to the ith particle the mass

$$\frac{g(x_i^0)}{N}.$$

Let these particles perform a random walk, keeping their mass fixed. Then after enough steps, the expected distribution of mass on the real line approximates (7).

In this process the total mass of the particles remains constant. This corresponds to the fact that

$$\partial_t \int_{-\infty}^{\infty} v(x,t)dx = \nu \int_{-\infty}^{\infty} v_{xx}(x,t)dx = 0$$

(assuming $v_x \to 0$ as $x \to \pm\infty$). Of course, one's intuitive feeling that the solutions of the heat equation decay is also correct. Indeed,

$$\partial_t \int_{-\infty}^{\infty} v^2(x,t)dx = \int_{-\infty}^{\infty} 2\nu v v_{xx}dx = -2\nu \int_{-\infty}^{\infty} (v_x)^2 dx < 0.$$

The decay of $\int v^2 dx$ (which occurs while $\int v\ dx$ remains constant) is accomplished by spreading. As time advances, the maxima of the solution decay and the variation of the solution decreases. To see intuitively why the integral of v^2 decreases, consider the two functions

$$v_1 = \begin{cases} 2, & -\frac{1}{2} \le x \le \frac{1}{2} \\ 0, & \text{elsewhere} \end{cases} \quad \text{and} \quad v_2 = \begin{cases} 1, & -1 \le x \le +1 \\ 0, & \text{elsewhere} \end{cases}$$

The function v_2 is more "spread out" than v_1. This is reflected by the calculations $\int v_2 dx = \int v_1 dx = 1$, but $\int v_2^2 dx = 2$ and $\int v_1^2 dx = 4$. Note that as time unfolds, the variance of the random walk that is used to construct the solution increases, whereas the integral of v^2, which is related to the variance of v, decreases. The variance of the random walk increases as the solution spreads out, whereas the integral of v^2 decreases because the range of values assumed by v decreases.

We now apply this algorithm to the Navier-Stokes equations. After each Euler step, we have to solve the heat equation $\xi_t = R^{-1}\Delta\xi$ for a time step Δt. This can be done by allowing each vortex to perform a random, gaussian jump of mean 0 and variance $2\Delta t/R$; thus, random pushes redistribute the vorticity and approximate diffusion.

Does one have to repeat the calculation over and over and then average? A simple calculation (that we omit, see [C4],[L4]) shows that the standard deviation of the value of the velocity field $\mathbf{u}$ at a point $\mathbf{x}$ (which is one estimate of the error) is proportional to $(RN)^{-1/2}$, where N is the number of vortices. If R and N are large, this is a small quantity, and a single realization (one calculation, one random push per particle per time step) is enough. Note however that in two space dimensions and in the absence of boundaries, the introduction of viscosity usually perturbs the solution only by an amount $O(R^{-1})$; thus

there is not much point in approximating viscous effects when R is large. The random method comes into its own when a boundary is present. Then the effect of viscosity is $O(1)$, while the error remains $O\left((RN)^{-1/2}\right)$, i.e., small.

Suppose for a moment the Euler step is performed by an explicit Euler integration. The equations of motion of the vortices are:

$$\mathbf{x}_i^{n+1} = \mathbf{x}_i^n + \mathbf{u}\Delta t + \sqrt{2/R}\,\mathbf{w},$$

where $\mathbf{x}_i^n \equiv \mathbf{x}_i(n\Delta t)$, Δt is the time step, and $\mathbf{w}$ is a two-component random variable, each component being gaussian with mean 0 and variance 1. In the limit $\Delta t \to 0$, this equation converges to the stochastic differential equation

$$d\mathbf{x} = \mathbf{u}dt + \sqrt{2/R}\,d\mathbf{w}, \tag{8}$$

where $d\mathbf{w}$ is "white noise", a gaussian random function of time with two independent components and no correlation between $\mathbf{w}(t_1), \mathbf{w}(t_2)$, $t_1 \neq t_2$. This equation (or more exactly, this set of equations, one per point in the support of ξ) is exactly equivalent to the Navier-Stokes equation (5) (see [C4],[L4]). In fact, the Navier-Stokes equation is the Fokker-Planck equation that corresponds to the stochastic differential equations (8). This means the following: one can propagate a probability density in time either by constructing samples and walking them at random (stochastic ordinary differential equations (8)), or by propagating the probability density of the particles (Navier-Stokes). The vorticity ξ plays the role of probability density; one would expect $\xi \geq 0$, $\int \xi d\mathbf{x} = 1$; the second condition can always be satisfied by an appropriate change of units (but it is not necessary to actually

do so), and the first can be achieved by dividing ξ into a positive part ξ_+ and a negative part ξ_-, and imagining that one is spreading them individually.

Equations (8) can be approximated without splitting, and thus one can construct unsplit random vortex methods, should one wish to.

In practice, all one has to do to approximate the Navier-Stokes in two dimensions in the absence of boundaries at large R is do nothing. If boundaries are present, all one has to do is add to the inviscid algorithm the appropriate gaussian jumps and of course satisfy the boundary conditions. Diffusion is particularly important near walls.

4. Boundary conditions.

Suppose the flow is bounded by solid walls. If $R^{-1} = 0$, the appropriate boundary condition (often $\mathbf{u} \cdot \mathbf{n} = 0$, where $\mathbf{n}$ is a normal to the boundary) is satisfied if G above is replaced by the Green function appropriate to the domain at hand. In practice, all one has to do is add to $\mathbf{u} = K * \xi$ a potential flow $\mathbf{u}_p$ such that their sum satisfies the boundary condition. $\mathbf{u}_p$ can be found by finite differences, or panel methods, or by images, or by conformal mapping. If $R^{-1} \neq 0$, the condition $\mathbf{u} \cdot \boldsymbol{\tau} = V_\tau$ must also be satisfied, where $\boldsymbol{\tau}$ is tangential to the boundary and V_τ is the tangential velocity of a solid boundary. In principle, all one has to do in this case is create a vortex sheet at the wall, with a strength calculated so as to annihilate unwanted deviations of $\mathbf{u} \cdot \boldsymbol{\tau}$ from its prescribed value (A vortex sheet is a tangential discontinuity in the velocity field; taking the curl at such a discontinuity produces vorticity supported by a line or "sheet"). The vorticity in the sheet diffuses into the fluid and participates in the subsequent motion; this process mimics the physical process of vorticity generation.

What is simple in principle is not necessarily so simple in practice. If one calculates with a finite time step Δt, and if at each time step one allows the vorticity to diffuse and be advected, the boundary condition $\mathbf{u}\cdot\boldsymbol{\tau} = V_\tau$ is satisfied exactly only at the beginning and at the end of each step, with local error that is at best $O(\sqrt{\Delta t})$ [C13]. One has to create some device to satisfy the boundary condition continuously. In the context of a blob method, this is done naturally by symmetry. For example, if the boundary is the x_1 axis, with the fluid in the $x_2 > 0$ half-plane, then one can continue the flow to the lower half-plane by the symmetry $\mathbf{u}(x_1, -x_2) = 2V_\tau - \mathbf{u}(x_1, x_2)$, guaranteeing $u_1(x_1, 0) = V_\tau$. Unfortunately, the Navier-Stokes equations are not invariant under this symmetry (consider what happens to $\xi = \partial_2 u_1 - \partial_1 u_2$), but the Prandtl equations $\xi_t + (\mathbf{u}\cdot\nabla)\xi = R^{-1}\partial_2^2\xi$, div $\mathbf{u} = 0$, that approximate them near walls, are invariant. The Prandtl equations have a blob representation [C5], and one can use the Prandtl blobs near walls, in a numerical boundary layer that should be thinner than any physical boundary layer, and then use a standard blob method in the interior.

Specifically, suppose the boundary corresponds to the x_1 axis, with the fluid occupying the half-plane $x_2 \geq 0$. The Prandtl boundary layer equations which approximate the Navier-Stokes equations near walls, are

$$\partial_t\xi + u_1\partial_1\xi + u_2\partial_2\xi = R^{-1}\partial_2^2\xi, \tag{9a}$$

$$\text{div } \mathbf{u} = 0, \tag{9b}$$

$$\xi = -\frac{\partial u}{\partial y}. \tag{9c}$$

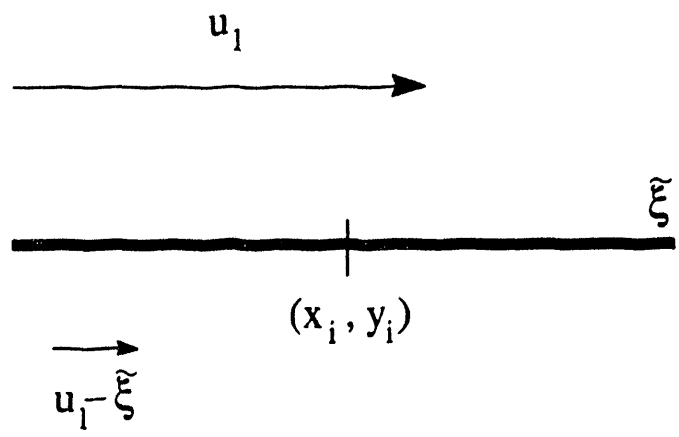

Fig. 1: A vortex sheet.

Note that the diffusion along the x_1 axis has disappeared, and the definition of vorticity has been simplified. These equations are invariant under the transformations $x_1 \rightarrow x_1$, $x_2 \rightarrow -x_2$, $u_1 \rightarrow -u_1$, $u_2 \rightarrow -u_2$, unlike the Navier-Stokes equations. The solution of equations (9) can be represented by a sum of vortex sheets of some finite length h, locations $\mathbf{x}_i$, and intensity $\tilde{\xi}_i$ [B5],[C5]. The boundary conditions for equations (9) are:

$$u_1 = u_2 = 0 \quad \text{at} \quad x_2 = 0,$$

$$u_1 = U \quad \text{at} \quad x_2 = \infty.$$

If the flow away from the boundary is inviscid, it can accept a normal boundary condition: $\mathbf{u} \cdot \mathbf{n}$ given; $\mathbf{u} \cdot \mathbf{n}$ will be produced by the numerical boundary layer. On the other hand, inviscid flow produces a tangential velocity at the wall as it pleases; this is the $u_1(x_2 = \infty) = U$ imposed on the sheets.

To move the sheets, one needs $\mathbf{u} = (u_1, u_2)$ at their centers. This will come from the Prandtl equations, rewritten as follows:

$$u_1(x_1, x_2) = U - \int_{x_2}^{\infty} \xi(x_1, s, t)ds, \qquad (\text{from } \partial_2 u_1 = -\xi)$$

$$u_2(x_1, x_2) = -\partial_1 \int_0^{x_2} u_1(x_1, s, t)ds, \qquad (\text{from } \mathbf{div}\mathbf{u} = 0).$$

In discrete form at the i-th sheet:

$$u_{1_i} = U - \frac{1}{2}\tilde{\xi}_i - \sum_j \xi_j d_j,$$

where $d_j = 1 - (|x_i - x_j|/h)$, and the sum $\sum_j$ is over all segments j such that $y_j > y_i$ and $|x_i - x_j| < h$ (so that $0 \le d_j \le 1$). The vertical velocity u_2 at the sheet i can then be approximated by

$$u_{2i} = -(I_1 - I_2)/h,$$

where I_1, I_2 approximate respectively $\int_0^{x_{2i}} u_1(x_i + h/2, s)ds$ and $\int_0^{x_{2i}} u_1(x_i - h/2, s)ds$, specifically

$$I_1 = Ux_{2i} - \sum_{j^+} \tilde{\xi}_j d_j^+ x_{2j}^*,$$

$$I_2 = Ux_{2i} - \sum_{j^-} \tilde{\xi}_j d_j^- x_{2j}^*,$$

where

$$d_j^+ = 1 - |x_{1i} + h/2 - x_{1j}|/h,$$

$$d_j^- = 1 - |x_{1i} - h/2 - x_{1j}|/h,$$

$$x_{2j}^* = \min(x_{2i}, x_{2j}),$$

and the sum $\sum_{j+}$ is over all sheets j such that $0 \leq d_j^+ \leq 1$, with $\sum_{j-}$ over all sheets such that $0 \leq d_j^- \leq 1$.

Given u_1, u_2 at the sheets, viscous diffusion can be approximated by adding to the x_2 component of the velocity the appropriate random jumps (gaussian, mean zero, variance $2\Delta t/R$). This procedure will automatically obey the boundary conditions $u_1 = U$ at infinity, $u_2 = 0$ at the wall.

To impose the condition $u_1 = 0$ at the wall, we create vorticity at the walls: divide the x_1-axis into segments of length h, and suppose that at the center P of one of these segments $u_1 \neq 0$. Place at P one or more vortex sheets, whose shadow is sufficient to make $u_1(P) = 0$. These sheets will then enter the flow by random walk and participate in the subsequent evolution. Since one can assume $\mathbf{u}(x_1, -x_2) = -\mathbf{u}(x_1, x_2)$, one can reflect any sheet that attempts to jump across the wall back into the flow. Note that the circulation attached to each sheet is $h\tilde{\xi}_i$.

The problem that remains is the correct matching of boundary blobs with standard blobs. An easy and workable solution is to transfer circulation from one type to the other across some line parallel to the wall, while matching the velocities parallel to the wall. This is usually good enough ([C2],[C5]). However, as is known from experience with matched asymptotic expansions, high accuracy requires a cleverer match. In particular, one should note that the velocity field induced by a Prandtl blob in its own neighborhood differs substantially from the velocity field induced by a standard blob, and the resulting mismatch of vertical velocities can deplete or overcrowd the vorticity in the transition zone and delay convergence. One would like an overlap between the numerical boundary

layer and the interior, and a match of both velocity components. For an appropriate construction, see [R2] and also [B7].

5. Fast summation.

At first glance, a time step in a blob method with N blobs requires $O(N^2)$ operations, a forbidding number if N is large. It turns out that the calculations can require far less effort, typically $O(N \log N)$ operations.

The key observation, as explained by Almgren et al. [A1], is that interactions that can be described by partial differential equations are overwhelmingly local. In particular, interactions described by a Green function for a Laplacian place a heavy emphasis on what happens when particles are near each other. For overall accuracy, it is enough if nearby interactions are calculated accurately, while distant interactions are calculated in a more global way, for example by conflating series or inverting an approximate Laplacian. Such partitioning schemes can be relatively inexpensive. Examples of algorithms that embody these observations are the local correction method [A1],[A2], the multipole expansion [G4], and other partitioning schemes [B1]. To explain the idea here, we pick a construction that is simple, elegant, and not very well known: Anderson's Poisson integration method [A3]. It can be viewed as a reformulation of the multipole method, and uses ideas developed by Rokhlin.

We consider the two-dimensional case (extension to three dimensions is reasonably straightforward). Diffusion does not affect the summation. To begin with, we consider point vortices, $\phi_\epsilon = \delta$; the extension to blobs is trivial. We thus have N point vortices, whose effect we wish to evaluate at N points. For simplicity, we shall write formulas as if

the object were to evaluate a stream function ψ; formulas for the velocity can be obtained by differentiation.

Suppose one has M vortices within a circle C of radius a and boundary ∂C, centered at the origin for ease of notation. Remember that two stream functions that are irrotational outside C, have the corresponding velocity fields vanish at infinity, and agree on ∂C, are identical. At a point (r, θ) outside C, ψ is given by

$$\psi(r,\theta) = \kappa \log r + \frac{1}{2\pi} \int_{\partial C} \psi(a,\theta) P(r,\theta') d\theta',$$

where κ is a constant and

$$P(r,\theta) = \left(1 - (a/r)^2\right) / \left(1 - 2(a/r)\cos(\theta - \theta') + (a/r)^2\right)$$

(the Poisson integration formula). The logarithmic term is written explicitly for convenience, and can be incorporated in the integral by adding a constant to $\psi(r, \theta)$. $\psi(a, \theta)$ is determined by the given vortices inside C. If the integral is approximated by a sum with K terms, $K \ll M$, and one wishes to calculate the ψ due to the M vortices at points outside C, then labor is saved. Accuracy for modest K normally requires equidistant integration nodes on ∂C.

A reminder of the derivation of the Poisson formula brings some useful insights. $\psi(r, \theta)$ can be expanded outside C in planar harmonics,

$$\psi(r,\theta) = \kappa \log r + \sum_{k=1}^{\infty} c_k \left(\frac{a}{r}\right)^k e^{ik\theta};$$

on $r = a$, this series reduces to a Fourier series, and thus the c_k can be found. A summation and an interchange of summation and integration yields (7). Note:

(i) Numerical integration mishandles high wave numbers, and thus for numerical purposes the expansion in planar harmonics need only be carried up to a finite number of terms. Summation and exchange of limits then produce a new kernel P_K that is better conditioned than P.

(ii) The error in the expansion, and thus in the use of the Poisson formula, depends only on $\psi(r,\theta)$ and on r/a, and is therefore scale invariant.

One then constructs a "tree structure" to evaluate the stream function on a succession of ever bigger circles, using circles of the preceding size to evaluate ψ on the circles of the next size level. Having done that, one goes down the ladder to evaluate ψ at the vortices: direct evaluation for nearby vortices, small circles for vortices a bit further apart, etc. The number of levels is $\sim \log N$, and the whole algorithm costs $O(N \log N)$ operations.

For more details, see [A3]; the general tree structure of fast summation is discussed in [K1]; parallel implementation is discussed in [S2].

6. The convergence of vortex methods (for the mathematically minded).

We now present a brief sketch of the convergence theory for vortex methods [B4],[B5],[C29],[H1],[H2],[R1], in the simplest case: two dimensions, $R^{-1} = 0$, ξ of compact support and no boundaries. The theory presented should be sufficient to illustrate the following points: (i) The error in vortex methods is primarily due to the error in the evaluation of the convolution integrals (4), and (ii) Accuracy depends on the properties of the smoothing ϕ, and can be enhanced by imposing on it certain moment conditions. The theory here should also give some of the flavor of the extensive and elegant body

of work that has arisen in this context. The presentation follows in the main references [A4],[C15],[C16].

Remember that the kernel K has been smoothed in the form: $K \to K_\epsilon$, $K_\epsilon = K * \phi_\epsilon$, $\phi_\epsilon = \epsilon^{-2}\phi(\mathbf{x}/\epsilon)$, $\int \phi d\mathbf{x} = 1$. Suppose ϕ is smooth enough (for precise requirements, see the references) and in addition, satisfies $\int \mathbf{x}^\alpha \phi(\mathbf{x}) d\mathbf{x} = 0$, where $\mathbf{x}^\alpha = x_1^{\alpha_1} x_2^{\alpha_2}$, $|\alpha| = \alpha_1 + \alpha_2$, and $0 < |\alpha| \leq p-1$ for some p, i.e., the moments of ϕ up to order $p-1$ vanish. The vortex method is written in the form (4): $d\tilde{\mathbf{x}}_i/dt = V_i(\tilde{\mathbf{x}})$, where $V_i(\mathbf{x}) = \sum_j \tilde{\xi}_j K_\epsilon(\mathbf{x}_i - \mathbf{x}_j)$.

Consider N blobs initially at $\boldsymbol{\alpha}_j$, $j = 1, \ldots, N$, where the $\boldsymbol{\alpha}_j$ are nodes of a regular square mesh of mesh size h placed on the support of ξ, and let $\tilde{\xi}_j = \xi(\boldsymbol{\alpha}_j)$. Let $\mathbf{x}_j(\boldsymbol{\alpha}_j, t)$ be the true trajectories issuing from the $\boldsymbol{\alpha}_j$, and $\tilde{\mathbf{x}}_j(\boldsymbol{\alpha}_j, t)$ the computed trajectories. Let $e_i(t) = x_i(\boldsymbol{\alpha}, t) - \tilde{x}_i(\boldsymbol{\alpha}, t)$, and for the sake of brevity, omit the subscript i from now on. $\dot{e} = \frac{de}{dt}$ satisfies

$$\begin{aligned} \dot{e} &= \dot{\mathbf{x}} - V(\tilde{\mathbf{x}}) \\ &= e_m + e_d + e_s, \end{aligned}$$

with

$$\begin{aligned} e_m &= \int K(\mathbf{x} - \mathbf{x}')\xi(\mathbf{x}')d\mathbf{x}' - \int K_\epsilon(\mathbf{x} - \mathbf{x}')\xi(\mathbf{x}')d\mathbf{x}' \\ e_d &= \int K_\epsilon(\mathbf{x} - \mathbf{x}')\xi(\mathbf{x}')d\mathbf{x}' - \sum_j K_\epsilon(\mathbf{x} - \mathbf{x}_j)\tilde{\xi}_j \\ e_s &= \sum_j K_\epsilon(\mathbf{x} - \mathbf{x}_j)\tilde{\xi}_i - \sum_j K_\epsilon(\tilde{\mathbf{x}}_i - \tilde{\mathbf{x}}_j)\tilde{\xi}_j. \end{aligned}$$

e_m is the "moment error" which arises because $K \to K_\epsilon$ (the origin of the name will become clear in a moment); e_d is the discretization error which results from the replacement of the integral by a sum; e_s is the "stability error" which arises because the sum is evaluated at the computed rather than the exact locations of the blobs. We shall now estimate these errors, noting that any integration over $\mathbf{x}$ or $\mathbf{x}'$ can be replaced by an integration

over $\boldsymbol{\alpha}$ or $\boldsymbol{\alpha}'$ (the Jacobian of the map $\boldsymbol{\alpha} \rightarrow \mathbf{x}$ being 1 by incompressibility); the grid in the integrations can thus be viewed as being regular even when the blob distribution has ceased to be regular as a result of the motion.

Let $g = g(x)$ be a function; we denote by $\hat{g}(k)$ its Fourier transform:

$$\hat{g}(k) = \int e^{i2\pi kx} g(x) dx;$$

then

$$g(x) = \int e^{-2\pi kx} \hat{g}(k) dk.$$

Note:

$$\hat{g}(0) = \int g(x) dx;$$

$$\widehat{f * g} = \hat{f}\hat{g};$$

(the Fourier transform of a convolution is the product of the Fourier transforms);

$$\widehat{(g(x/\epsilon))} = \epsilon \hat{g}(\epsilon k);$$

(this scaling property is actually the mathematical statement of the Heisenberg uncertainty principle of quantum mechanics); and finally,

$$\widehat{\left(\frac{d}{dx} g\right)} = -2\pi i k \hat{g}.$$

We defined $e_m = K * \xi - K_\epsilon * \xi$; Thus

$$\begin{aligned} \hat{e}_m(\mathbf{k}, t) &= (\hat{K} - \hat{K}_\epsilon)\hat{\xi}, \\ &= \hat{K}(1 - \hat{\phi}_\epsilon)\hat{\xi}, \\ &= \hat{K}\hat{\xi}\left(\hat{\phi}(0) - \hat{\phi}(\epsilon \mathbf{k})\right), \end{aligned}$$

since $1 = \int \phi d\mathbf{x} = \hat{\phi}(0)$. The moment condition guarantees that the derivatives of orders up to $p-1$ of $\hat{\phi}$ are zero, and straightforward manipulation yields $\| e_m \|_{L^1} \leq$ constant $\cdot \epsilon^p$.

To estimate e_d, we shall first exhibit some inequalities which prove the high order accuracy of trapezoidal rule integration for sufficiently smooth integrands. Elementary considerations show that if $\mathbf{i} = (i_1, i_2)$ is a pair of integers, $\mathbf{i} = 0$ if $i_1 = 0$, $i_2 = 0$, and $\| \mathbf{i} \| = \max(|i_1|, |i_2|)$, then for $L \geq 3$, $\sum_{\mathbf{i} \neq 0} \| \mathbf{i} \|^{-L} \leq 16$. Suppose $g = g(x_1, x_2) \in C_0^r$, and define $\| g \|_r = \max(\| \partial^r g \|_{L^1})$ (the maximum of the L^1 norms of all the derivatives of g up to order r). Then, for $r \geq 3$,

$$\left| \sum_{\mathbf{i}} g(\mathbf{i}h) - \int g(\mathbf{x}) dx \right| \leq \frac{12}{(2\pi)^r} \| g \|_r \, h^r$$

(trapezoidal rule integration is very accurate). Indeed, by the Poisson summation formula [D1],

$$h^2 \sum_{\mathbf{i}} g(\mathbf{i}h) = \sum_{\mathbf{i}} \hat{g}(\mathbf{i}/h),$$

where $\hat{g}$ is the Fourier transform of g. Therefore,

$$\left| h^2 \sum_{\mathbf{i}} g(\mathbf{i}h) - \int g(\mathbf{x}) d\mathbf{x} \right| = \left| \sum \hat{g}(\mathbf{i}h) - \hat{g}(0) \right| = \left| \sum_{\mathbf{i} \neq 0} \hat{g}(\mathbf{i}/h) \right|.$$

Also, $|\hat{g}| \leq \int |g(\mathbf{x})| d\mathbf{x}$, and $\widehat{\partial^\alpha g}(\mathbf{k}) = (2\pi i)^{|\alpha|} k^\alpha \hat{g}(k)$, where $\partial^\alpha = \partial_1^{\alpha_1} \partial_2^{\alpha_2}$, $|\alpha| = \alpha_1 + \alpha_2$, and $k^\alpha = k_1^{\alpha_1} k_2^{\alpha_2}$; thus

$$|(2\pi)^r k^r \hat{g}| \leq \int |\partial^r g| d\mathbf{x} \leq \| g \|_r \, .$$

Then

$$|\hat{g}(\mathbf{k})| \leq \frac{\| g \|_r}{(2\pi)^r} \frac{1}{\| \mathbf{k} \|^r},$$

and for $r \geq 3$,

$$\left| \sum_{\mathbf{i} \neq 0} \hat{g}(i/h) \right| \leq \left| \frac{\| g \|_r}{(2\pi)^r} \sum_{\mathbf{i} \neq 0} \| \mathbf{i}/h \|^{-r} \right| \leq \frac{16}{(2\pi)^r} \| g \|_r h^r.$$

To estimate e_d, all we need is an estimate for the derivatives of $K_\epsilon = K * \phi_\epsilon$. K_ϵ has as many derivatives as ϕ has, and if ϕ has L derivatives, a straightforward analysis yields at finite time T:

$$\max_{0 \leq t \leq T} \| e_d \|_{L^\infty} \leq \text{constant} \cdot \left(\frac{h}{\epsilon} \right)^L \cdot \epsilon.$$

We omit the analysis of e_s, which can be bounded in such a way that the over-all error is bounded by a constant times $(\| e_d \| + \| e_m \|)$; thus

$$\| \text{error} \|_{L^1} \leq \text{constant} \left(\epsilon^p + \left(\frac{h}{\epsilon} \right)^L \epsilon \right).$$

(Note the usefulness of a finite ϵ.) If L is large enough, one can choose $h/\epsilon < 1$ (thus making the blobs overlap) so that the error in the trajectories of the blobs is close to $O(h^p)$. We omit the discussion of how one goes from trajectory error to other measures of the error, and how one accounts for the effects of time discretization. For error estimates in the presence of viscosity or in three dimensions, see the references.

One key to accuracy (or more precisely, to local accuracy, see below) in blob methods is to satisfy the moment conditions $\int \mathbf{x}^\alpha \phi d\mathbf{x} = 0$ for α as large as possible. (An appropriate choice of ϕ can produce "spectral" accuracy [H2] but other methods are needed for the analysis.)

As an example, consider $\phi(\mathbf{x}) = \frac{1}{\pi} e^{-r^2}$, where $r = |\mathbf{x}|$. Clearly, $\int \phi d\mathbf{x} = 1$, $\int x_1 \phi d\mathbf{x} = \int x_2 \phi d\mathbf{x} = 0$, so that $p = 2$. If $\phi(\mathbf{x}) = e^{-r^2} - \frac{1}{2} e^{-r^2/2}$, one can check that $p = 4$ [B5]. Generally, one can construct appropriate ϕ's by picking plausible forms

with free coefficients and picking the coefficients so as to satisfy the moment conditions. The construction of the appropriate K_ϵ is easy: $K_\epsilon = \left(\begin{smallmatrix}\partial_2\\ -\partial_1\end{smallmatrix}\right) G_\epsilon$, where $G_\epsilon = G * \phi_\epsilon$. $\Delta G_\epsilon = \Delta(G * \phi_\epsilon) = (\Delta G) * \phi_\epsilon = \phi_\epsilon$, where Δ is the Laplace operator $\partial_1^2 + \partial_2^2$, and the rules for manipulating convolutions given in section 2 are used. If $\phi = \phi(r)$, $\Delta = r^{-1}\frac{d}{dr}\left(r\frac{d}{dr}\right)$, and thus, if $\phi = \frac{1}{\pi}e^{-r^2}$, $\phi_\epsilon = \frac{1}{\pi\epsilon^2}e^{-r^2/\epsilon^2}$, $r^{-1}\frac{d}{dr}\left(r\frac{d}{dr}G_\epsilon\right) = \frac{1}{\pi\epsilon^2}e^{-r^2/\epsilon^2}$, $\frac{d}{dr}G_\epsilon = \frac{1}{2\pi r}\left(e^{-r^2/\epsilon^2} - 1\right)$, $K_\epsilon = \frac{(-y,x)}{2\pi r^2}\left(1 - e^{-r^2/\epsilon^2}\right)$; the vortex method becomes

$$\frac{dx_i}{dt} = \sum_{i\neq j} \frac{-(y_i - y_j)}{2\pi r_{ij}^2}\left(1 - e^{-r_{ij}^2/\epsilon^2}\right)$$

$$\frac{dy_i}{dt} = \sum_{i\neq j} \frac{(x_i - x_j)}{2\pi r_{ij}^2}\left(1 - e^{-r_{ij}^2/\epsilon^2}\right),$$

where for convenience I wrote $x = x_1$, $y = x_2$, $r_{ij} = |\mathbf{x}_i - \mathbf{x}_j|$. An expansion of the smoothing factor $\left(1 - e^{-r_{ij}^2/\epsilon^2}\right)$ in power series shows that the singularity at $r_{ij} = 0$ is cancelled out. Similarly, if $\phi = e^{-r^2} - \frac{1}{2}e^{-r^2/2}$,

$$K_\epsilon = \frac{(-y,x)}{2\pi r^2}\left(1 - 2e^{-r^2/\epsilon^2} + e^{-r^2/2\epsilon^2}\right).$$

The analysis shows that a good choice for the $\mathbf{x}_i(0)$, $\tilde{\xi}_i$, is one that makes the integration in $K_\epsilon * \xi$ accurate; the $\mathbf{x}_i$ should be on a regular grid and the $\tilde{\xi}_i$ should be the appropriate point values.

The error in blob method does grow in time. One factor in this exponential growth is the growing irregularity of the blob distribution and the resulting growth in the derivatives that enter the error in a trapezoidal rule. This growth can be remedied by periodic rezoning (see e.g. [N4]). By construction, the "polygonal" methods mentioned above perform a rezoning at each time step, and as a result the errors they produce often grow less rapidly.

Other limitations on long-time accuracy will be discussed in the next few sections.

7. Vortex methods in three space dimensions.

In three space dimensions, vortex methods are a little more difficult to formulate, because the vorticity is now a divergence-free vector whose magnitude changes [C5],[K3],[L2],[L3]. The Euler equations take the forms

$$\partial_t \boldsymbol{\xi} + (\mathbf{u} \cdot \nabla)\boldsymbol{\xi} = -(\boldsymbol{\xi} \cdot \nabla)\mathbf{u}, \tag{10}$$

$$\text{div } \mathbf{u} = 0;$$

$\boldsymbol{\xi} = \text{curl } \mathbf{u}$ is the vorticity. The two-dimensional relation between $\boldsymbol{\xi}$ and $\mathbf{u}$ can be generalized: div $\mathbf{u} = 0$ makes it possible to write $\mathbf{u} = \text{curl } \mathbf{A}$, $\mathbf{A}$ = vector potential, which can be chosen so that div $\mathbf{A} = 0$. Then

$$\boldsymbol{\xi} = \text{curl curl } \mathbf{A} = -\Delta \mathbf{A}, \qquad \Delta = \sum \partial_j^2,$$

and

$$A = -\frac{1}{4\pi} \int \frac{1}{|\mathbf{x} - \mathbf{x}'|} \boldsymbol{\xi}(\mathbf{x}') d\mathbf{x}', \qquad d\mathbf{x}' = dx_1' dx_2' dx_3'$$

where $-(4\pi r)^{-1}$ is the Green function of the Δ operator, $-\Delta(4\pi r)^{-1} = \delta(\mathbf{x} - \mathbf{x}')$, δ = delta function. Taking the curl, one obtains

$$\mathbf{u} = K * \boldsymbol{\xi},$$

where $K = -\left(4\pi|\mathbf{x}|^3\right)^{-1} \times$, $\times$ denoting a cross-product, and $*$ is a convolution as before; in other symbols,

$$\mathbf{u}(\mathbf{x}) = -\frac{1}{4\pi} \int \frac{(\mathbf{x} - \mathbf{x}') \times \boldsymbol{\xi}(\mathbf{x}')}{|\mathbf{x} - \mathbf{x}'|^3} d\mathbf{x}'. \tag{11}$$

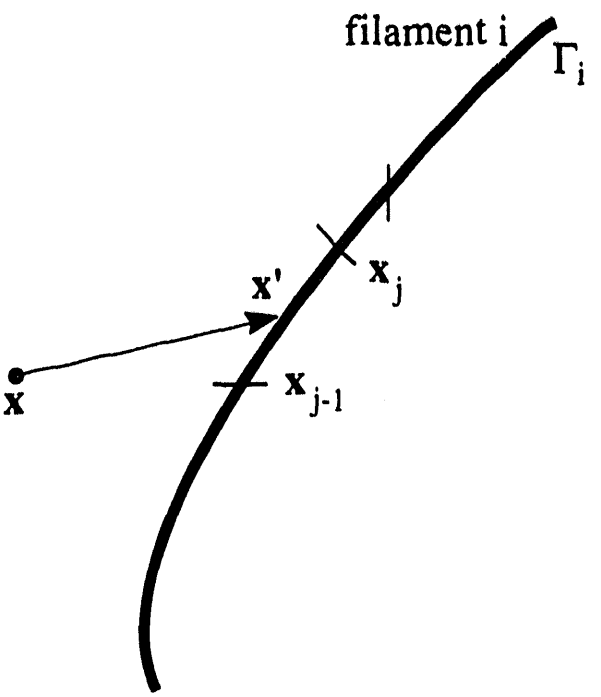

XBL 937-4069

Fig. 2: A vortex filament.

This is the "Biot-Savart" law. The first approximation one can make is to replace $\xi(\mathbf{x})$ by a collection of vortex lines (lines tangent at each point to $\boldsymbol{\xi}$), and concentrate the vorticity on these lines. If $\boldsymbol{\xi}$ is smooth enough, the lines will be closed. div $\boldsymbol{\xi} = 0$ means that the flux of vorticity along such lines is a constant; let the i-th line have a flux Γ_i; then (fig. 2)

$$\mathbf{u}(\mathbf{x}) = -\frac{1}{4\pi}\sum_i \Gamma_i \int_{\text{along } i\text{-th line}} \frac{(\mathbf{x}-\mathbf{x}')\times d\mathbf{s}}{|\mathbf{x}-\mathbf{x}'|^3}.$$

It is easy to see that this expression typically becomes singular near the filaments, so that one has to replace $K = -\left(4\pi|\mathbf{x}-\mathbf{x}'|^3\right)^{-1}\mathbf{x}\times$ by a smoother object K_ϵ, or alternatively,

smear the lines into "filaments". The integration along the lines can be done numerically, so that for example

$$\mathbf{u}(\mathbf{x}) = -\frac{1}{4\pi}\sum_i \Gamma_i \sum_j \frac{(\mathbf{x}-\mathbf{x}_j)\times(\mathbf{x}_j-\mathbf{x}_{j+1})}{|\mathbf{x}-\mathbf{x}_j|^3},$$

where the $\mathbf{x}_j$ are points along the i-th line. K_ϵ can again be obtained in the form

$$K_\epsilon = K * \phi_\epsilon, \quad \phi_\epsilon = \epsilon^{-3}\phi(\mathbf{x}/\epsilon),$$

where $\int \phi d\mathbf{x} = 1$, $\int x_1^{\alpha_1} x_2^{\alpha_2} x_3^{\alpha_3} \phi d\mathbf{x} = 0$ for $\alpha_1 \geq 0, \alpha_2 \geq 0, \alpha_3 \geq 0, \alpha_1+\alpha_2+\alpha_3 \leq p-1$ for some integer p. A standard example of an appropriate ϕ is the fourth-order Beale-Majda smoothing function ($p = 4$) [B4], which leads, as before, to a smoothed kernel,

$$K_\epsilon = \left(1 + \left(\frac{3}{2}\tilde{r}^3 - 1\right)e^{-\tilde{r}^3}\right) K, \quad \tilde{r} = |\mathbf{x}|/\epsilon;$$

it is easy to check that the factor will cancel the singularity of K at small $r = |\mathbf{x}|$. Note that the "stretching" term on the right-hand side of equation (10) is not explicitly represented; its effect is to stretch vortex lines when there is a velocity gradient along them; this is automatically done by allowing the points along the filaments to move at different speeds. The velocity field $\mathbf{u}$ can then be used to move the points $\mathbf{x}_i$. This is the "vortex filament" method.

Tracking whole filaments may pose some bookkeeping problems. One can extract from the filaments segments such as $\overline{x_{j-1}x_j}$ (fig. 2) and follow their end-points without reference to the rest of the filament. div $\boldsymbol{\xi} = 0$ will be satisfied if the calculation is accurate enough [B3],[C6]. This is the "arrow", or "segment", or "vorton" method. Diffusion and boundary conditions are easy to handle in this way, but div $\boldsymbol{\xi} = 0$ requires some care and possibly a

periodic extraction of the divergence-free part of the vorticity field. (See the next section, and the review [W5].) In both the filament and the arrow methods, additional points must be added as the vortex lines stretch [C7],[K3]. An interesting discussion of boundary conditions can be found in [S5].

Other variants are possible: one may for example keep track only of the mid-point of a segment, and account for vortex stretching by updating $\boldsymbol{\xi}$ through an evaluation of $-(\boldsymbol{\xi} \cdot \nabla)\mathbf{u}$. An additional major variant is discussed in the next section.

An inviscid vortex method in three space dimensions can usually be run only for a finite time, just as is the case with other inviscid methods. The physics of fluid flow bring energy to the small scales. Sooner or later there will not be enough vortex elements to represent the "eddies" being created, and the time step will be too small to follow the small scale rotation. This loss of resolution usually manifests itself as excess folding of vortex lines. Folding is a physical phenomenon (vortex lines stretch, as the stretch they must fold or else energy will increase [C8],[C13],[C16]). Excess folding is a problem.

There are several remedies: one can stop the calculation when folding becomes excessive. One can add diffusion by non-random means, something people are loath to do; having gone to the trouble of making an inviscid method, they do not like the idea of adding viscosity. The final possibility is renormalization: the replacement of the unrepresented eddies by their effect on the remaining eddies. An appropriate vortex renormalization requires statistical ideas that will be discussed in the following section. In brief, statistical analysis suggests that it is legitimate to filter out small vortex loops.

It is interesting to note that vortex calculations in three dimensions, with a high accuracy core, are usually first undone by the lack of accuracy in the time integration. This is unusual; in other methods, it is the lack of spatial accuracy that will get you first. The explanation seems to be as follows: the energy transfer to small scales is produced by vortex stretching; stretching cannot be uniform in space without energy increase [C8],[C11]; as a result, vortex activity concentrates in small very active regions (a phenomenon known as "intermittency"). Computational vortex elements can follow this concentration, not being tied to a grid, thus easing the problem of spatial resolution but placing an added burden on the time integration, which must represent accurately rotations in small volumes. In general, other methods, if only they could provide enough spatial resolution, would also eventually stumble on the time integration problem.

Applications of three-dimensional vortex methods can be found i.a. in [C7],[G1],[K4],[K5],[L3].

8. The impulse/magnet representation.

At this point, the character of these lectures is changing. From the realm of reasonably tried and true, we are jumping into the speculative and hopeful. First, we present a variant of three-dimensional vortex methods that is not well tested but has exceptional physical interest, and then we proceed to vortex statistics and to speculations about turbulence and superfluids.

A short preliminary: If $\mathbf{u}$ is defined in a domain $\mathcal{D}$, with $\mathbf{u} \cdot \mathbf{n} = 0$ on the boundary $\partial\mathcal{D}$ and div $\mathbf{u} = 0$, and if grad ϕ is any gradient, then $\int_{\mathcal{D}} \mathbf{u} \cdot \text{grad } \phi = \int_{\mathcal{D}} \phi \text{div } \mathbf{u} = -\int_{\partial\mathcal{D}} \mathbf{u} \cdot \mathbf{n} = 0$; $\mathbf{u}$ and grad ϕ are orthogonal in function space. Any vector $\mathbf{w}$ can then

be uniquely written as $\mathbf{w} = \mathbf{u}_d + \text{grad } \phi$, where $\mathbf{u}_d$ satisfies $\mathbf{u}_d \cdot \mathbf{n} = 0$ on $\partial\mathcal{D}$, div $\mathbf{u}_d = 0$. The $\mathbf{u}_d$ is the divergence-free part of $\mathbf{w}$; $\mathbf{u}_d$ can be viewed as the result of an orthogonal projection P, $\mathbf{u}_d = P\mathbf{w}$; we have: $P^2 = P$, P grad $\phi = 0$ for any ϕ, $P\mathbf{u}_d = \mathbf{u}_d$. The Navier-Stokes equations can be written in the form

$$\mathbf{u}_t = P\left(-(\mathbf{u}\cdot\nabla)\mathbf{u} + R^{-1}\Delta\mathbf{u}\right).$$

This observation is the key to projection methods (see Prof. Ferziger's course and reference [C7]).

It is well known that in an appropriate abstract sense Euler's equations, in both two and three space dimensions, form a Hamiltonian system. We have exhibited a Hamiltonian structure in two space dimensions through the use of vortices. Hamiltonian formulations are not unique; once one has been found others can be derived from it.

In three space dimensions, one specific Hamiltonian formulation that seems to have been discovered independently by several investigators, has been shown by Buttke [B8] to lead to discrete systems with remarkable properties. The starting point is the introduction of a new variable, $\mathbf{m}$, often referred to rather awkwardly as a magnetization, or vortex magnetization, or impulse (for reasons we shall see), obtained by adding to $\mathbf{u}$ at some point in time an arbitrary gradient:

$$\mathbf{m} = \mathbf{u} + \text{grad } q \qquad \text{at } t = 0. \tag{12}$$

Obviously at $t = 0$, $\mathbf{u} = P\mathbf{m}$, with the projection P defined above. It is not required that div $\mathbf{m} = 0$. We have $\boldsymbol{\xi} = \text{curl } \mathbf{u} = \text{curl } \mathbf{m}$. If one thinks of $\mathbf{u}$ as the vector potential of $\boldsymbol{\xi}$, (12) is a gauge transformation of the kind that allows one to add a gradient to the

magnetic vector potential in electromagnetic theory without changing the physics. q is not unique, nor is $\mathbf{m}$.

We now proceed in a non-intuitive fashion to find equations for the evolution of $\mathbf{m}$. The end result of our analysis should be heuristically transparent and will justify the effort. We only consider the case of an unbounded domain $\mathcal{D}$.

Consider the following equation for evolving $\mathbf{m} = (m_1, m_2, m_3)$:

$$\frac{Dm_i}{Dt} \equiv \partial_t m_i + u_j \partial_j m_i = -m_j \partial_i u_j \tag{13}$$

(with summation over multiple indices, and $\mathbf{u} = P\mathbf{m}$). The claim is that the resulting $\mathbf{u}$ is identical to the solution of Euler's equations if $\mathbf{u}(\mathbf{x}, 0) = P\mathbf{m}(\mathbf{x}, 0)$. Equation (13) is then the gauge-invariant form of Euler's equations. For the sake of simplicity, we assume there are no external forces.

To check the claim, substitute $\mathbf{m} = \mathbf{u} + \text{grad}\, q$ into (13). After some elementary manipulations, one obtains

$$\partial_t \mathbf{u} + (\mathbf{u} \cdot \nabla)\mathbf{u} = -\text{grad}\left(\partial_t q + (\mathbf{u} \cdot \nabla)q + \frac{1}{2}|\mathbf{u}|^2\right). \tag{14}$$

Multiplication by the projection P yields

$$\partial_t \mathbf{u} + P\left((\mathbf{u} \cdot \nabla)\mathbf{u}\right) = 0, \tag{15}$$

as promised. Conversely, one can start from equation (15), which is equivalent to Euler's equations, and obtain (13). Note that multiplication of (14) by $(I - P)$ (I = identity operator) yields an equation for the evolution of q, which is thus arbitrary only at $t = 0$. It follows from (12) that $\mathbf{m}$ and $\mathbf{u}$ always differ by a gradient.

We now have an equation for the evolution of $\mathbf{u}$ plus an initially arbitrary gradient. We shall put this gradient to good use.

Suppose $\boldsymbol{\xi} = \text{curl } \mathbf{u}$ has support within a ball B of finite radius ρ. In three space dimension, the exterior of a sphere is simply connected, and thus outside B one can write $\mathbf{u} = -\text{grad } \tilde{q}$. put $q = \tilde{q}$ in (12). The resulting $\mathbf{m}$ has support in B. $\mathbf{m}$ can thus be "localized", and this localization persists in time.

Suppose $\boldsymbol{\xi}$ has support in a small sphere B_ϵ; calculate the resulting $\mathbf{m}$ so that $\mathbf{m}$ also has support in B_ϵ,

$$\mathbf{m} = \mathbf{M}\phi_\epsilon(\mathbf{x} - \mathbf{x}_i);$$

$\mathbf{x}_i$ is a point in B_ϵ, $\mathbf{M}$ is a vector coefficient, and $\phi_\epsilon(\mathbf{x} - \mathbf{x}_i)$ is, as before, a smooth function, with supp ϕ_ϵ in B_ϵ, $\int \phi_\epsilon(\mathbf{x})d\mathbf{x} = 1$. The resulting $\mathbf{u}$ differs from $\mathbf{M}\phi_\epsilon(\mathbf{x}-\mathbf{x}_i)$ by a gradient:

$$\mathbf{u} - \mathbf{M}\phi_\epsilon = K * (\text{curl } \mathbf{M}\phi_\epsilon) - \mathbf{M}\phi_\epsilon = \text{grad } q,$$

and thus div $\mathbf{M}\phi_\epsilon = -\Delta q$, Δ = Laplace operator. Some manipulation of vector identities yields q and then

$$u_i = M_i\phi_\epsilon(\mathbf{x} - \mathbf{x}_i) - M_j\partial_j\partial_i\psi_\epsilon, \tag{16}$$

where $\psi_\epsilon = \psi_\epsilon(\mathbf{x} - \mathbf{x}_i)$ satisfies $\Delta\psi_\epsilon = \phi_\epsilon$.

Consider an arbitrary magnetization field $\mathbf{m}$ and write it as a sum of N function of small support ("magnets") of the type we have just described:

$$\mathbf{m} = \sum_{i=1}^{N} \mathbf{M}^{(i)}\phi_\epsilon(\mathbf{x} - \mathbf{x}_i).$$

The motion of the "centers" $\mathbf{x}_i$ of these functions is of course given by

$$\frac{d\mathbf{x}_i}{dt} = \mathbf{u}(\mathbf{x}_i) = \sum_{j=1}^{N} \mathbf{u}^{(j)}(\mathbf{x}_i), \tag{17}$$

where $\mathbf{u}^{(j)}$ is the velocity (16) due to the j-th "magnet". The coefficients $\mathbf{M}^{(i)}$ are not constants; from equation (13) one finds

$$\frac{dM_i^{(k)}}{dt} = -M_j^{(k)} \partial_i u_j(\mathbf{x}_k), \tag{18}$$

where there is summation over repeated indices and the u_j are the components of $\mathbf{u} = \sum \mathbf{u}^{(k)}$.

One can now check that the flow of these "magnets" is Hamiltonian, with

$$\begin{aligned} H &= \tfrac{1}{2} \textstyle\sum_j \mathbf{M}^{(j)} \cdot \mathbf{u}(\mathbf{x}_j) \\ &= \tfrac{1}{2} \textstyle\sum_{j=1}^{N} \sum_{i=1}^{N} \left[\mathbf{M}^{(i)} \cdot \mathbf{M}^{(j)} \phi_\epsilon(\mathbf{x}_i - \mathbf{x}_j) + (\mathbf{M}^{(i)} \cdot \nabla_i)(\mathbf{M}^{(j)} \cdot \nabla_j) \psi_\epsilon(\mathbf{x}_i - \mathbf{x}_j) \right] \end{aligned}, \tag{19}$$

where $\nabla_j = (\partial_{x_{j1}}, \partial_{x_{j2}}, \partial_{x_{j3}})$, $\mathbf{x}_j = (x_{j1}, x_{j2}, x_{j3})$, and $\Delta \psi_\epsilon = \phi_\epsilon$. If at $t = 0$ the $\mathbf{x}_j$ are distributed so that the sum in (19) approximates an integral,

$$H \sim \frac{1}{2} \int \mathbf{m} \cdot \mathbf{u} d\mathbf{x} = \frac{1}{2} \int (\mathbf{u} + \text{grad } q) \cdot \mathbf{u} d\mathbf{x} = \frac{1}{2} \int \mathbf{u}^2 d\mathbf{x},$$

i.e., the kinetic energy is indeed a Hamiltonian for the flow if one uses the appropriate variables.

One can check that the equations

$$\frac{dx_{jk}}{dt} = \frac{\partial H}{\partial M_k^{(j)}}, \quad \frac{dM_k^{(j)}}{dt} = -\frac{\partial H}{\partial x_{jk}}, \quad (\mathbf{x}_j = (x_{j1}, x_{j2}, x_{j3})),$$

are exactly equation (17) and (18).

The "magnets" $\mathbf{M}\phi_\epsilon$ have a simple interpretation. One can check, by a painful but elementary calculation, that the velocity field (16) is the velocity field induced by a small vorticity loop with $\mathbf{M}$ perpendicular to the plane of the loop, and $|\mathbf{M}| = \Gamma A$, where A is the area of the loop and Γ is the circulation. We have thus approximated $\boldsymbol{\xi}$ by a sum of small vortex loops.

There is an analogy between magnetostatics and fluid dynamics, in which the current corresponds to vorticity and the magnetic induction corresponds to velocity; the magnetostatic variables are related by the Biot-Savart law just like the fluid variables. In this analogy, our $\mathbf{m}$ corresponds to the magnetization, hence the name.

The loop interpretation shows how to convert a vortex representation to a loop representation. Consider a large vortex loop C of circulation Γ. Construct a surface Σ that spans C. The non-uniqueness of Σ corresponds to the non-uniqueness of q and $\mathbf{m}$. Let (s_1, s_2) be orthogonal coordinates on Σ. Construct a small rectangle $\mathcal{R}$ with vertices (s_1, s_2), $(s_1 + \delta s_1, s_2)$, $(s_1, s_2 + \delta s_2)$, $(s_1 + \delta s_1, s_2 + \delta s_2)$; at its center construct a small magnet of strength $\Gamma \delta s_1 \delta s_2$, oriented in a direction orthogonal to Σ chosen consistently. The sum of these loops adds up to the original loop.

It is easy to check that $\mathbf{m}$ remains orthogonal to Σ as both are evolved by the flow map. This construction points out a problem with the $\mathbf{m}$ representation: A vortex loop will eject fluid to its rear and thus Σ will balloon; as its area increases so does $\sum |\mathbf{M}_j|$; as a result the time steps may become small and the calculation expensive. Appropriate remaps to remedy this problem have been considered by Cortez [C14]. The magnetization representation has

not yet been tested as a sufficient number of examples for firm conclusions about its usefulness to be drawn.

The magnet/impulse representation is "local" like the "arrow" representation; div $\boldsymbol{\xi} = 0$ automatically; diffusion is easy to add; smoothness has been built in from the beginning (it was necessary to keep all quantities bounded). This representation is a key component of some theoretical treatments of turbulence [C11].

Note that for thin closed vortex filaments lying in a plane,

$$\Gamma \int \mathbf{x} \times ds = 2A\Gamma,$$

where A is the area surrounded by the filament. Thus

$$\int \mathbf{x} \times \boldsymbol{\xi} d\mathbf{x} = 2 \int \mathbf{m} d\mathbf{x}$$

and $2\mathbf{m}$ is an "impulse density"; note that impulse density is thus non-unique. It follows that $\int \mathbf{m} d\mathbf{x}$ is a constant of the motion; one can indeed check that $\Sigma \mathbf{M}^{(k)}$ is a constant of the motion for the system (17)–(18), as is the sum

$$\sum \mathbf{x}_k \times \mathbf{M}^{(k)},$$

which is analogous to an angular momentum.

9. Statistical mechanics of vortices in the plane.

We start the statistical analysis by considering N vortices in a bounded region $\mathcal{D}$ in two dimensions. The entropy S of the system is the logarithm of the density of its states (the Boltzmann constant can be set equal to 1 by using appropriate units). The temperature T is defined by $T^{-1} = dS/d\langle E\rangle$, where $\langle E\rangle$ is the average of the energy E. If the system has states labelled by a parameter s, then $S = -\sum_s P_s \log P_s$, where P_s is the probability of the state s and the sum is to be interpreted as an integral when the states form a continuum. In the canonical ensemble, $P_s = Z^{-1}\exp(-E/T)$, where $E = E(s)$ is the energy of the state labelled by s and Z is a normalizing constant, the "partition function" $Z = \sum P_s$.

One is used to having $T > 0$, but this inequality is not a law of nature. One can perfectly well imagine systems such that for $\langle E\rangle$ moderate there are many ways of arranging their components so that the energy adds up to $\langle E\rangle$ but for $\langle E\rangle$ large there are only a few ways of doing so. Then the derivative $dS/d\langle E\rangle$ is negative for $\langle E\rangle$ large enough and T is negative. This situation will indeed occur for vortex systems. If $T > 0$ low energy states have a high probability, and if $T < 0$ high energy states have a high probability.

Suppose one takes two systems, each separately in equilibrium, one with energy E_1 (we drop the brackets) and entropy S_1, the other with energy E_2 and entropy S_2. Suppose one joins them; the resulting union has energy E_1+E_2 and is not necessarily in equilibrium. Its entropy, initially $S = S_1 + S_2$, will increase in time t. Then

$$\frac{dS}{dt} = \frac{dS_1}{dt} + \frac{dS_2}{dt} = \frac{dS_1}{dE_1}\frac{dE_1}{dt} + \frac{dS_2}{dE_2}\frac{dE_2}{dt} > 0,$$

while energy is conserved:

$$\frac{dE_1}{dt} + \frac{dE_2}{dt} = 0.$$

Therefore

$$\frac{dS}{dt} = \left(\frac{dS_1}{dE_1} - \frac{dS_2}{dE_2}\right)\frac{dE_1}{dt} = \left(\frac{1}{T_1} - \frac{1}{T_2}\right)\frac{dE_1}{dt}.$$

Suppose $T_2 > T_1$, both positive; then $\frac{dE_1}{dt} > 0$, i.e., energy moves from the hotter body to the colder body. Now suppose $T_2 < 0$. It still follows that $\frac{dE_1}{dt} > 0$, i.e. a body with negative temperature is "hotter" than a body with positive temperature. Negative temperatures are above $T = \infty$, rather than below absolute zero. Further, the canonical formula shows that $T = -\infty$ is indistinguishable from $T = +\infty$; $|T| = \infty$ is the boundary between $T < 0$ and $T > 0$. In terms of $\beta = T^{-1}$, temperature increases as β varies from infinity to zero through positive values, and then from zero to minus infinity through negative values.

Consider a collection of N vortices of small support occupying a finite portion $\mathcal{D}$ of the plane, of area $A = |\mathcal{D}|$ (see [E1]). The area can be made finite by surrounding it with rigid boundaries, in which case the vortex Hamiltonian must be modified through the addition of immaterial smooth terms; alternatively, one can confine the vortices to a finite area initially and conclude that they will remain in a finite area, because the center of vorticity $\mathbf{X} = \Sigma\tilde{\xi}_i\mathbf{x}_i/\Sigma\tilde{\xi}_i$, $\mathbf{x}_i$ = positions of the vortices, and the angular momentum $\Sigma\tilde{\xi}_i^2|\mathbf{x}_i - \mathbf{X}|^2$, are invariant. For the moment, consider inviscid flow with all the $\tilde{\xi}_i = 1$. The entropy of this system is

$$S = -\int_{\mathcal{D}^N} f(\mathbf{x}_1, \ldots, \mathbf{x}_N) \log f(\mathbf{x}_1, \ldots, \mathbf{x}_N) d\mathbf{x}_1 d\mathbf{x}_2 \cdots d\mathbf{x}_N,$$

where f is the probability that the first vortex is in a small neighborhood of $\mathbf{x}_1$, the second in a small neighborhood of $\mathbf{x}_2$, etc. The energy of this system is $E = H + B$, where H is the two-dimensional vortex Hamiltonian and B is an appropriate constant. The entropy is maximum when

$$f = \text{constant} = A^{-N}.$$

The corresponding energy is

$$\langle E \rangle = \langle E_c \rangle = -\frac{1}{4\pi} N(N-1) \int_{\mathcal{D}} d\mathbf{x} \int_{\mathcal{D}} d\mathbf{x}' \log |\mathbf{x} - \mathbf{x}'| + B.$$

Clearly, one can produce a larger $\langle E \rangle$ by bunching vortices together, and thus $T^{-1} = dS/dE < 0$ for $E > \langle E_c \rangle$. This is Onsager's observation. If $T > 0$, the Gibbs factor $\exp(-E/T)$ gives a high probability to low energy states, and if $T < 0$, high energy states are favored; the latter are produced by bunching together vortices, forming large, concentrated vortex structures. The $f = \text{constant}$ state is the $|T| = \infty$ boundary between $T < 0$ and $T > 0$. The T introduced here has no connection whatsoever with the molecular temperature of the underlying fluid; in incompressible flow, the molecular degrees of freedom and the vortex variables are insulated from each other.

To give this argument a more quantitative form, we turn to the elementary combinatorial method [J1]. We assume there are N vortices. N^+ vortices have strength $\tilde{\xi} = 1$, N^- have $\tilde{\xi} = -1$, $N^+ + N^- = N$. We divide $\mathcal{D}$ into M boxes of area h^2, with n_i^+ positive and n_i^- negative vortices in each. The corresponding probability (= multiplicity) W is

$$W = \left(\frac{N^+!}{n_1^+! \ldots n_M^+!} \right) \left(\frac{N^-!}{n_1^-! \ldots n_M^-!} \right) h^{2N}.$$

To a good approximation, the entropy is $S = \log W$ (for the conditions under which this is true, see e.g. [E1],[C11]). To obtain an equilibrium, S is to be maximized subject to the constraints $\Sigma n_i^+ = N^+$, $\Sigma n_i^- = N^-$, and

$$E = \frac{1}{2}\sum_i \sum_{j\neq 1} (n_i^+ - n_i^-) G_{ij} (n_j^+ - n_j^-) = \text{constant},$$

where $G_{ij} = -\frac{1}{2\pi}\log|\mathbf{x}_i - \mathbf{x}_j| + B$, $\mathbf{x}_i$ is in the i-th box, $\mathbf{x}_j$ is in the j-th box, and B is a constant. This E approximates the energy of a vortex system. The maximization of S produces a thermal equilibrium and leads to the equations

$$\begin{aligned} \log n_i^+ + \alpha^+ + \beta \textstyle\sum_j G_{ij}(n_j^+ - n_j^-) &= 0, \\ \log n_i^- - \alpha^+ + \beta \textstyle\sum_j G_{ij}(n_j^+ - n_j^-) &= 0, \end{aligned} \tag{20}$$

where $\alpha^+, \alpha^-, \beta$ are Lagrange multipliers. A little algebra yields

$$\begin{aligned} n_i^+ - n_i^- = & \quad \exp\left(-\alpha^+ - \beta \textstyle\sum_j G_{ij}(n_j^+ - n_j^-)\right) \\ & - \exp\left(-\alpha^- + \beta \textstyle\sum_j G_{ij}(n_j^+ - n_j^-)\right), \end{aligned}$$

for $i = 1, \ldots, M$. Let $h \to 0$ so that $n_i^+ - n_i^- \to \xi(\mathbf{x})h^2 = \xi(\mathbf{x})d\mathbf{x}$, $(\exp(-\alpha^-))/h^2 \to d^-$, and $\Sigma G_{ij}(n_i^+ - n_i^-) \to \int G(\mathbf{x}-\mathbf{x}')\xi(\mathbf{x}')d\mathbf{x}'$, where $G(\mathbf{x}) = -\frac{1}{2\pi}\log|\mathbf{x}| + B$. Equations (20) converge to

$$\xi(\mathbf{x}) = d_+ \exp(+\beta \int G(\mathbf{x}-\mathbf{x}')\xi(\mathbf{x}')d\mathbf{x}') + d_- \exp(-\beta \int G(\mathbf{x}-\mathbf{x}')\xi(\mathbf{x}')d\mathbf{x}')$$

where d_+, d_- are appropriate normalization coefficients.

Let ψ be the stream function, $u_1 = -\partial_2\psi$, $u_2 = \partial_1\psi$; an easy calculation gives $\Delta\psi = -\xi$, Δ = Laplace operator and $\psi = -\int G(\mathbf{x}-\mathbf{x}')\xi(\mathbf{x}')d\mathbf{x}'$. Thus,

$$-\Delta\psi = \xi(\mathbf{x}) = d_+ e^{-\beta\psi} - d_- e^{\beta\psi}. \tag{21}$$

This is the Joyce-Montgomery equation, which describes the vortex version of thermal equilibrium. In a periodic domain one can set $\psi = 0$ on the boundary of a period; $N^+ = N^- = N/2$, $d_+ = d_- = d$. Then

$$2d = \frac{N}{\int d\mathbf{x} e^{\beta\psi}},$$

$$-\Delta\psi(\mathbf{x}) = \xi(\mathbf{x}) = d \sinh \beta\psi(\mathbf{x}).$$

If $N^+ = N$, $N^- = 0$, then $d_- = 0$, $d^+ = N/Z$, $Z = \int_{\mathcal{D}} e^{-\beta\psi} d\mathbf{x}$, and

$$-\Delta\psi = \xi(\mathbf{x}) = \frac{N}{Z} \exp\left(\beta\psi(\mathbf{x})\right).$$

In either case, ξ is a function of ψ. The Euler equation is

$$\begin{aligned} \partial_t \xi &= -u_1 \partial_1 \xi - u_2 \partial_2 \xi \\ &= (\partial_2\psi)(\partial_1\xi) - (\partial_1\psi)(\partial_2\xi) = J(\psi, \xi), \end{aligned}$$

where J = Jacobian of ξ, ψ which is zero when $\xi = \xi(\psi)$. The resulting average flow is a stationary (time-independent) solution of the Euler equation, with macroscopic motion, as expected when $\beta < 0$. Appropriate variants of equation (21) can be derived, in which the limit $N \to \infty$ can be easily taken [E1],[K2],[M2].

It should be emphasized that the ξ we have calculated is not only a specific solution of Euler's equation, but more importantly it is the stationary average density of the vorticity. Specific flows may depart from this average, but one expects the departure to be small.

For $\beta \geq 0$ and for $-8\pi N < \beta < 0$ equation (21) can be shown to have solutions. In the latter case the solutions are non-unique; the solutions have multiple peaks; the solution that maximizes the entropy has a single sharp but smooth peak. For $\beta < -8\pi N$ (i.e., "hotter" than $T = -1/8\pi N$), the Joyce-Montgomery equation with $\xi \geq 0$ has no classical solution and in fact does not describe reasonable physics.

Statistical equilibria are of interest only if they are reached from most initial data. There is strong evidence, mainly numerical, that the two-dimensional equilibria constructed above are in fact reached. Some general statements can be made about the relaxation to equilibrium, and some equations remain open.

Suppose one starts from initial data that consist of two patches of vorticity, say $\xi = 1$ in sets C_1, C_2, both bounded, C_1, C_2 disjoint, and $\xi = 0$ elsewhere. Since vorticity is merely transported by the fluid motion, one has to imagine a process by which the vorticity in the patches is redistributed so as to match ξ_∞, the solution of the one-sign Joyce-Montgomery equation (21). One can imagine that the boundaries of C_1, C_2 sprout filaments, as in the convergence of subsets of the constant energy surface to the microcanonical ensemble; the resulting filaments could reorganize so as to approximate ξ_∞ on a sufficiently crude scale.

The filamentation of the boundary should lower the energy. Indeed, if a small vortex patch is broken into two halves that are pulled apart, the energy goes down; two vortices of strength $\tilde{\xi} = 1$ each, near each other, act as one vortex of strength 2, whose energy is four times that of one of them; two vortices of strength 1 far from each other have an energy that is the sum of their individual energies. To make up for the loss of energy in filamentation the two patches have to approach each other. This process of simultaneous filamentation and consolidation is well documented numerically. Similarly, one expects a non-circular patch to become nearly circular with a halo of filaments, the whole approximating ξ_∞ on a rough scale. Even a circular patch with non-constant ξ, increasing from its center outward, can reorganize its vorticity so that filaments shoot off while energy is being conserved. On the other hand, a patch with ξ decreasing as one moves away from the center is stable,

and belongs to the set of initial data that do not approach ξ_∞; such a patch of course does in itself constitute a rough version of ξ_∞.

This process of simultaneous filamentation and consolidation can be deduced from the invariance of the energy and the enstrophy in spectral form: $\int E(k)dk = \text{constant}$, $\int k^2 E(k)dk = \text{constant}$, where $E(k)$ is the energy spectrum. If some energy moves towards the large k's (small scales), then even more energy must move towards the small k's (large scales). On the whole, there is an energy "cascade" toward the small k's.

If the initial ξ is complicated, and has many maxima and minima, one can imagine, and indeed see on the computer, a process of progressive curdling, in which nearly circular patches that look locally like ξ_∞ first form on small scales, then slowly migrate towards each other and consolidate if viewed on a crude enough scale. The curdles can never truly merge, since the flow map is one-to-one. At each stage of this curdling the nearly circular patches are nearly independent, with whatever correlations their locations have manifesting itself only on large scales. The flow can then be approximated as $\Sigma \eta_i \xi_\infty(\mathbf{x} - \mathbf{x}_i)$, $\eta_i =$ random coefficients. The energy spectrum is approximately proportional to $|\mathbf{k}|^2 |\hat{\xi}_\infty(\mathbf{k})|^2$, where $\hat{\xi}_\infty$ is the Fourier transform of $\xi_\infty(\mathbf{x})$, and is a property of each curd individually. One then has local equilibria slowly consolidating into larger equilibria.

This successive curdling picture provides a suggestion as to what happens in the presence of shear or in complex geometries. In three space dimensions the "universal" aspects of turbulence appear on small scales, and one can readily imagine that arbitrary large scale structures have "universal" small scale features. Here, in two dimensions, the universal structures grow to large scales, and an imposed shear or an imposed boundary

mass interferes with them. It is readily imagined however that the curdling process will simply stop when it ceases to be compatible with the conditions imposed on the problem.

Note that if ϕ_ϵ in the two-dimensional vortex method is identified with ξ_∞, then the vortex method can be reinterpreted as a model of two-dimensional turbulence, in which the smallest scales have reached equilibrium. Indeed, this is how the ϕ_ϵ in [C3],[C4] was chosen.

One can wonder about the effect of a small viscosity ν on the processes just described. To the extent that the effect of viscosity is to smear the small scales, and as long as the time it takes to reach equilibrium is small compared to the time scale of viscous decay, the picture above should be unaffected. One could say a little more: suppose the effect of viscosity is approximated by Brownian motion (equation (8)). The Brownian motion can be thought of as being generated by the bombardment of the vortices by the molecules of an ambient fluid at a temperature ν. The effect of the bombardment that has just been imagined is to couple weakly the "fluid" at the temperature ν with the vortex system, and if $\nu < T =$ vortex temperature, to reduce the latter. If $T < 0$, the cooling of the vortex system brings one closer to the $|T| = \infty$ equidistribution solution, in agreement with the intuitive idea that random pushes should interfere with the formation of concentrated vortices. After a long enough time one may end up with $\xi =$ constant.

10. Statistics of vortex filaments in three dimensions.

We now turn to the three-dimensional analogues of the constructions of the previous section. In three dimensions, vortex filaments are extended objects, more like polymers than like particles; vortex stretching is important, and only a statistically steady state can

be expected as the time $t \to \infty$. To make the presentation easy, we consider a single vortex filament (a tight bunch of integral lines of the vorticity field) in a dilute "suspension" of such filaments; more general situations are considered in [C9],[C11].

Suppose our filament can be covered by N nearly circular cylinders, each of length $h > 0$. Endow the filament with an energy

$$E = \frac{\Gamma^2}{8\pi} \sum_i \sum_{j \neq i} \frac{\mathbf{t}_i \cdot \mathbf{t}_j}{|i-j|} \tag{22}$$

where $\mathbf{t}_i$ is a vector of length h originating at the center of the i-th cylinder, $|i-j|$ is the distance between the i-th and j-th cylinders, and Γ is the circulation of the vortex. Equation (22) is the discrete analogue of the Lamb expression for the energy [L1]:

$$E = \frac{1}{2} \int \mathbf{u}^2 d\mathbf{x} = \frac{1}{8\pi} \int d\mathbf{x} \int d\mathbf{x}' \frac{\boldsymbol{\xi}(\mathbf{x}) \cdot \boldsymbol{\xi}(\mathbf{x}')}{|\mathbf{x} - \mathbf{x}'|}.$$

The vortex is self avoiding: $|\mathbf{x} - \mathbf{x}'| \neq 0$ for $\mathbf{x} \in$ the i-th cylinder, $\mathbf{x}' \in$ the j-th cylinder.

Assume that each configuration C of the vortex has probability $P(C) = Z^{-1} \exp(-E/T)$, where $Z = \sum_C P(C)$. T can be positive or negative; "increasing T" is defined as in the previous section. The average energy $\langle E \rangle = \sum_C E(C)P(C)$ is an increasing function of both T and vortex length $L = Nh$.

Define

$$\mu_{N,T} = \frac{\log \langle r_N \rangle}{\log N},$$

where r_N is the end-to-end length of the vortex measured by a straight ruler. As $N \to \infty$, $\mu_{N,T}$ tends to a limit μ_T; $1/\mu_T$ is the fractal dimension of the resulting limiting object [C13],[C16].

For fixed, finite N, $\frac{\partial \mu_{N,T}}{\partial T} < 0$; i.e., as T decreases, the vortex becomes an increasingly folded object. In the limit $N \to \infty$, $\mu_T = 1$ for $T < 0$, $\mu_T = 1/3$ for $T > 0$, $\mu_T \cong .59$ for $|T| = \infty$. Note that $|T| = \infty$ is the maximum entropy state.

Suppose now that the "vortex" is imbedded in an Euler flow. Its length will increase, by stretching and by fractalization; $\frac{dN}{dt} < 0$. The average energy is an increasing function of both T and of the vortex length L. If energy is conserved, it follows that $\frac{dN}{dt} < 0$ and the temperature decreases. Also, $\frac{d\mu_{N,T}}{dt} < 0$ and the vortices fold, as described at the end of section 5. If the vortex is initially smooth, $T(t = 0) < 0$, and the temperature decreases to $|T| = \infty$. The point $|T| = \infty$ is an attracting fixed point for Euler dynamics; that is where the vortices will end up and generate a Kolmogorov spectrum [C11]. $|T| = \infty$ is an uncrossable barrier for Euler dynamics. Asymptotic vortex structures are poised at the boundary between $T > 0$ and $T < 0$.

Note that as long as N is finite, strong, organized, coherent structures contribute less to the energy dissipation than weaker, incoherent vortices. Indeed, contrast two vortex filaments with the same finite N but different circulations Γ_1, Γ_2, say $\Gamma_1 > \Gamma_2$. The energy integral being proportional to Γ^2, the Gibbs weights attached to the two filaments are $Z^{-1}\exp(-\beta\Gamma_1^2 E)$, $Z^{-1}\exp(-\beta\Gamma_2^2 E)$, where E is the energy that results from $\Gamma = 1$. These weights are the same as those one would obtain with $\Gamma = 1$ and $T_1 = T/\Gamma_1^2$ in the first case, $T_2 = T/\Gamma_2^2$ in the second. If one thinks of $D = 1/\mu_{N,T}$ as an approximate fractal dimension, the vortex with larger Γ has a smaller $|T|$, and if $T < 0$ (which is the physically relevant case), then the vortex with larger Γ has a smaller dimension and appears smoother.

Strong vortices are less folded. The more folded vortex has a broader spectrum and thus contributes more to dissipation relative to its energy.

In a numerical calculation, N remains finite, and the $|T| = \infty$ barrier can be crossed. If it is, excess folding and stretching may follow, as is indeed observed. One can reduce this excess by a systematic removal of folds ("hairpins") which can be justified as a renormalization [C10]. Hairpin removal is a very useful tool in vortex methods.

The justification of the removal goes like this: suppose $T \gtrsim 0$. The probability of a state with energy E is $\sim e^{-E/T}$. If a large loop is given, the smaller loops will, as a consequence, arrange themselves so as to reduce the energy. If the smaller loops are removed, the energy of the system must be increased to make up for the loss. On the other hand, if $T < 0$, large energy states are more likely, a given loop tends to align smaller loops so as to increase the energy, and this must be allowed for if small loops are removed. At $|T| = \infty$ the effect of small loops on large loops is, on the average, zero. Thus the small loops can be removed, sometimes removing energy from the system, and sometimes adding energy to the system, with a balance being reached for a large enough system. It only remains to notice that a large loop with a fold can be viewed as the sum of a large loop and a small loop.

There may however be simpler ways to arrest the crossing of the $|T| = \infty$ barrier. A key observation in this respect is Qi's observation [Q1] that the crossing is most likely to happen where the vortex torsion is zero; such points are readily identifiable before disaster strikes.

11. Remarks on turbulence and on superfluid vortices.

In the previous section we developed a theory of thermal equilibria of vortex filaments and used it to explain the folding instability of computational vortex filaments. The theory can also be applied directly to physical vortices.

In a classical (i.e., non quantum) fluid in turbulent motion vortex filaments typically form a dense suspension; their cross-sections vary rapidly and play a role in the dynamics. The equilibrium theory of filaments is a plausible cartoon of the equilibrium states of vortex filaments in this context, and reveals important features of the motion; it must however be interpreted with some care [C11].

A major conceptual leap that must be made in order to apply the model to turbulence concerns the idea that the inertial range of turbulence can be described by an equilibrium model. In the usual presentation of the Kolmogorov theory, inertial scales do little besides transfer energy from large to small scales, in an irreversible waterfall-like cascade that cannot be assimilated to a thermal equilibrium. However, there is overwhelming experimental [M5] and numerical [C11] evidence that energy goes both up and down the ladder of scales; in other problems, even in Burgers' equation, equilibrium and a power law spectrum appear together. An equilibrium with a wide spectrum may enhance dissipation, but not necessarily be dominated by it. This argument is laid out in detail in [C11]. In superfluid (quantum) turbulence these arguments are easier to visualize. In a superfluid, vortices exist as physical entities; their cores are well defined. The dissipation mechanisms (e.g., the Hall-Vinen friction [H3]) do not concentrate at the smallest scales and the simple cascade ideas are not as attractive. Indeed, "fractal" vortex equilibria similar to the ones

described above do occur, for example, near the T_λ transition to superfluidity [S3],[W2] or in the related problem of "vortex glasses" in "high temperature" superconductors [H6].

However, some paradoxes appear as soon as one considers turbulence in superfluids more closely. In many important respects, quantum and classical turbulence are very different. Quantum vortices generally look smoother than classical vortices. The rate at which quantum vortex length per unit volume L is generated appears to be proportional to $L^{3/2}w$, where w is a quantum "counterflow" velocity that vanishes in a non-superfluid. By contrast, the rate of change of L in classical turbulence is proportional to L [C11]. Thus vortex stretching appears to be much more important in classical than in quantum turbulence.

A qualitative explanation of these differences is contained in the theory of the last section. The rate of change of L was connected with the rate of change of the temperature T. A classical fluid has a self-adjusting temperature T such that $|T| \to \infty$, and there are no bounds on L. In a quantum fluid (and maybe also in compressible turbulence) wave/vortex interactions control T and then L may be bounded. Deeper explanations remain to be explored; the relations of quantum to fluid vortex motion are discussed in [C9],[C11]. Vortex methods appear as the natural tools for analyzing these relations and the structure of turbulence in general.

This may be the place to dwell on a numerical mystery. If vortex stretching and folding are inhibited in quantum turbulence, vortex motion in quantum and classical fluids should be very different. In a partial recognition of this fact, superfluid physicists often replace the Biot-Savart law (9) by a different velocity fluid that depends only on a local curvature of

the vortex filament. The equations obtained from this approximation, the "local induction approximation" (LIA) have a very different character from the Euler equations, and in particular they preserve vortex length [B6],[C6]. It is however persistently claimed in the superfluidity literature that the LIA and the Biot-Savart law can be used interchangeably.

In one case, examined by Buttke [B6], it turns out that the resemblance between the LIA and the Euler results claimed in earlier work is an artifact of the numerics; a sufficient refinement of the mesh in the LIA destroys this resemblance. There are however more subtle problems. For example, according to recent work [S1], waves propagate on vortex filaments with only a "confined chaos" and no breakdown of the vortex. A crude enough solution of the Euler equations in this case reproduces the results of the LIA to a good approximation. A more resolved calculation is at sharp variance with the LIA, but an even more refined calculation produces again results that have a qualitative (but not quantitative) similarity to the results obtained by the LIA [Q1]. A deeper understanding of this situation is not yet available.

12. Acknowledgment

This work was supported in part by the Applied Mathematical Sciences Subprogram of the Office of Energy Research, U.S. Department of Energy under Contract DE-AC03-76SF00098.

References

The literature on vortex methods has become very large; references [A5], [C1],[C11],[G4],[M1],[M2],[M3],[R1] and [P1] contain extensive bibliographies. I have listed below only those references that are used in the text. I apologize to all the authors whose work is omitted and assure them that no value judgement is implied.

[A1] A. Almgren, T. Buttke and P. Colella, A fast vortex method in three dimensions, J. Comp. Phys., 1993, in press.

[A2] A. Anderson, A method of local corrections for computing the velocity field due to a distribution of vortex blobs, J. Comput. Phys., 61, 111–123 (1985).

[A3] C. Anderson, An implementation of the fast multipole method without multipoles, SIAM J. Sc. Stat. Comp.; 13, 923–947 (1992).

[A4] C. Anderson and C. Greengard, On vortex methods, SIAM J. Sc. Stat. Comp., 22, 413–440 (1985).

[A5] C. Anderson and C. Greengard, Vortex methods, Lecture notes in mathematics, Springer, vol. 1360, 1988.

[B1] J. Barnes and P. Hut, A hierarchical $O(N \log N)$ force calculation algorithm, Nature, 324, 446–449 (1986).

[B2] J.T. Beale and A. Majda, Vortex methods I: Convergence in three dimensions, Math. Comp.,39,1–27 (1982).

[B3] J.T. Beale and A. Majda, Vortex methods II: Higher order accuracy in two and three space dimensions, Math. Comp., 32, 29–52 (1982).

[B4] J.T. Beale and A. Majda, High order accurate vortex methods with explicit velocity kernels, J. Comp. Phys.., 58, 188–208 (1985).

[B5] G. Benfatto and M. Pulvirenti, A diffusion process associated with the Prandtl equation, J. Funct. Anal., 52, 330–343 (1983).

[B6] T. Buttke, Numerical study of superfluid turbulence in the self- induction approximation, J. Comp. Phys., 76, 301–326 (1988).

[B7] T. Buttke, A fast adaptive vortex method for patches of constant vorticity in two dimensions, J. Comp. Phys., 89, 161–186 (1990).

[B8] T. Buttke, Lagrangian numerical methods which preserve the Hamiltonian structure of incompressible fluid flow, Comm. Pure Appl. Math., 1993, in press.

[C1] R. Caflisch, Mathematical analysis of vortex dynamics, SIAM, Philadelphia, 1988.

[C2] A. Cheer, Unsteady separated wake behind an impulsively started cylinder, J. Fluid Mech., 201, 485–505 (1989).

[C3] A.J. Chorin, Vortex methods for rapid flow, Proc. 2d Int. Cong. Num. Meth. Fluid Mech., Springer, 1972.

[C4] A.J. Chorin, Numerical study of slightly viscous flow, J. Fluid Mech., 57, 785–796 (1973).

[C5] A.J. Chorin, Vortex models and boundary layer instability, SIAM J. Sc. Stat. Comp., 1, 1–21 (1980).

[C6] A.J. Chorin, The evolution of a turbulent vortex, Comm. Math. Phys., 83, 517–535 (1982).

[C7] A.J. Chorin, Computational fluid mechanics, selected papers, Academic, 1989.

[C8] A.J. Chorin, Statistical mechanics and vortex motion, AMS lectures in applied mathematics, 28, 85–101 (1991).

[C9] A.J. Chorin, A vortex model with turbulent and superfluid percolation, J. Stat. Phys., 69, 67–78 (1992).

[C10] A.J. Chorin, Hairpin removal in vortex interactions II, J. Comput. Phys., 107, 1-9 (1993)

[C11] A.J. Chorin, Vorticity and Turbulence, Springer, 1993.

[C12] A.J. Chorin and P. Bernard, discretization of a vortex sheet with an example of roll-up, J. Comp. Phys., 13, 423–429 (1973).

[C13] A.J. Chorin and J. Marsden, A mathematical introduction to fluid mechanics, Springer, 1979, 1990.

[C14] R. Cortez, The geometry of impulse flow, Manuscript, Math. Dept, UC Berkeley, 1993.

[C15] G.H. Cottet, Methodes particulaires pour l'equation d'Euler dans le plan, These de 3ieme cycle, Univ. P. and M. Curie, Paris, 1982.

[C16] G.H. Cottet, A new approach to the analysis of vortex methods in two and three space dimensions, Ann. Inst. H. Poincare, Anal. Non Lin., 5, 227–285 (1988).

[C17] G.H. Cottet, Large time behavior for deterministic particle approximations to the Navier-Stokes equations, Math. Comp., 56, 45–60 (1991).

[D1] H. Dym and H. McKean, Fourier series and integrals, Academic, 1972.

[E1] G.L. Eyink and H. Spohn, Negative temperature states and equivalence of ensembles for the vortex model of a two-dimensional ideal fluid, J. Stat. Phys., 70, 833–886 (1993).

[F1] D. Fishelov, A new vortex scheme for viscous flow, J. Comput. Phys., 86, 211–224 (1990).

[G1] A.F. Ghoniem and G. Heidarinejad, Numerical study of scalar mixing and product formation in a shear layer, Combust. Sci. Tech., 72, 79–99 (1990).

[G2] J. Goodman, The convergence of random vortex methods, Comm. Pure Appl. Math., 40, 189–220 (1987).

[G3] L. Greengard and V. Rokhlin, A fast algorithm for particle simulations, J. Comput. Phys., 73, 325–348 (1988).

[G4] K. Gustafson and J. Sethian, Vortex methods and vortex flows, SIAM, 1991.

[H1] O.H. Hald, Convergence of vortex methods II, SIAM J. Sc. Stat. Comp., 16, 726–755 (1979).

[H2] O.H. Hald, Convergence of vortex methods for Euler's equations III, SIAM J. Num. Anal., 24, 538–582 (1987).

[H3] H. Hall and W. Vinen, The rotation of liquid Helium II: The theory of mutual friction, Proc. Roy. Soc. London, A 238, 215–233 (1956).

[H4] T.Y. Hou and J. Lowengrub, Convergence of a point vortex method for the 3D Euler equations, Comm. Pure Appl. Math., 43, 965–981 (1990).

[H5] T.Y. Hou and B. Wetton, Convergence of a finite difference scheme for the Navier-Stokes equations using vorticity boundary conditions, SINUM 29, 615–639 (1992).

[H6] D. Huse, M. Fisher and D. Fisher, Are superconductors really superconducting? Nature, 358, 553–559 (1992).

[J1] G. Joyce and D. Montgomery, Negative temperature states for the two-dimensional guiding center plasma, J. Plasma Physics, 10, 107–121 (1973).

[K1] J. Katzenelson, Computational structure of the N-body problem, SIAM J. Sc. Stat. Comp., 10, 787–815 (1989).

[K2] M. Kiessling, Statistical mechanics of classical particles with logarithmic interactions, Comm. Pure Appl. Math., 1993, in press.

[K3] O. Knio and A. Ghoniem, Three dimensional vortex methods, J. Comp. Phys., 86, 75–106 (1990).

[K4] O.M. Knio, and A.F. Ghoniem, Three-dimensional vortex simulation of the rollup and entrainment in a periodic shear layer, J. Comput. Phys., 97, 172–223 (1991).

[K5] O.M. Knio and A.F. Ghoniem, The three-dimensional structure of periodic vorticity layers under non-symmetric conditions, J. Fluid Mechanics, 243, 353–392 (1992).

[K6] R. Krasny, Desingularization of periodic vortex sheet roll-up, J. Comput. Phys., 65, 292–289 (1986).

[K7] R. Krasny, A study of singularity formation in a vortex sheet by the point vortex approximation, J. Fluid Mech., 167, 65–93 (1986).

[L1] H. Lamb, Hydrodynamics, Dover, NY, 1932.

[L2] A. Leonard, Numerical simulation of interacting three-dimensional vortex filaments, Proc. 4th Int. Conf. Num. Meth. Fluids, Springer, 1975.

[L3] A. Leonard, Computing three dimensional vortex flows with vortex filaments, Ann. Rev. Fluid Mech., 17, 523–559 (1985).

[L4] D.G. Long, Convergence of the random vortex method in two dimensions, J. Am. Math. Soc., 1, 779–804 (1988).

[M1] A. Majda, Vorticity and the mathematical theory of incompressible fluid flow, Comm. Pure Appl. Math., 39, S187–S179 (1986).

[M2] A. Majda, Vorticity, turbulence and acoustics in fluid flow, SIAM Review, 33, 349–388 (1991).

[M3] C. Marchioro and M. Pulvirenti, Vortex methods in two- dimensional fluid mechanics, Springer, NY, 1984.

[M4] L.-F. Martins and A.F. Ghoniem, Vortex simulation of the flow field in a planar piston-chamber arrangement with an intake, Int. J. for Num. Meth. Fluids., 12, 237–260 (1991).

[M5] C. Meneveau, Dual spectra and mixed energy cascade of turbulence in the wavelet representation, Phys. Rev. Lett., 66, 1450–1453 (1991).

[P1] E.G. Puckett, A review of vortex methods, in "Incompressible computational fluid mechanics", R. Nicolaides and M. Ginzburger (eds.), Cambridge, 1992.

[Q1] A. Qi, Three dimensional vortex methods for the analysis of propagation on vortex filaments, Ph.D. thesis, Math. Dept., UC Berkeley, 1991.

[R1] P. Raviart, An analysis of particle methods, Num. Meth. Fluid Mech., F. Brezzi (ed.), Springer, 1985.

[R2] M. Reider, Development of higher order numerical methods for two-dimensional incompressible flow with applications to flow around circular cylinders and airfoils, Ph.D. thesis, Math. Dept., UCLA, 1992.

[R3] L. Rosenhead, The formation of vortices from a surface of discontinuity, Proc. Roy. Soc. London, A 134, 170–192 (1931).

[R4] G. Russo and J. Strain, Fast triangulated vortex methods for the 2D Euler equations, J. Comput. Phys., 1993, in press.

[S1] D. Samuels, and R. Donnelly, Sideband instability and recurrence of Kelvin waves on vortex cores, Phys. Rev. Lett., 64, 1385–1388 (1990).

[S2] J. Sethian, J.P. Brunet, A. Greenberg and J. Mesirov, Two dimensional viscous incompressible flow in complex geometry on a massively parallel processor, J. Comput. Phys., 101, 185–206 (1992).

[S3] S.R. Shenoy, Vortex loop scaling in the three-dimensional XY ferromagnet, Phys. Rev. B, 40, 5056–5068 (1989).

[S4] D. Summers, A random vortex simulation of Falkner-Skan boundary layer flow, J. Comput. Phys., 85, 86–103 (1989).

[S5] D. Summers, An algorithm for vortex loop generation, LBL report, Lawrence Berkeley Lab., 1992.

[W1] G. Winckelmans and A. Leonard, Contributions to vortex particle methods for the computation of three-dimensional incompressible unsteady flow, J. Comput. Phys., 1993, in press.

[W2] G. Williams, Vortex ring model of the superfluid lambda transition, Phys. Rev. Lett., 59, 1926–1929 (1987).

DATE
FILMED
1/26/94
END